

1
2
3
4
5
6
7
8
9
10
11
12
13
14
15
16
17
18
19
20
21
22
23
24
25
26
27
28

Hox11-expressing interstitial cells contribute to adult skeletal muscle at homeostasis

Corey G.K. Flynn¹, Qingyuan Guo², Paul R. Van Ginkel¹, Steven M. Hrycaj³, Aubrey E. McDermott¹, Angelo Madruga¹, Deneen M. Wellik^{1*}

¹Department of Cell and Regenerative Biology, University of Wisconsin School of Medicine and Public Health, Madison, WI 53705

²Cell and Molecular Biology Program, University of Wisconsin-Madison, Madison, WI 53705

³Department of Pathology, University of Michigan, Ann Arbor, MI 48109

*Correspondence: wellik@wisc.edu

Corresponding Author:

Deneen M. Wellik, PhD
Department of Cell & Regenerative Biology
University of Wisconsin-Madison
School of Medicine and Public Health
1111 Highland Avenue
4405 WIMR II
Madison, WI 53705
608-262-5491

29 **Summary Statement**

30 Hoxa11 expression marks a novel population of muscle interstitial cells capable of
31 extensive, satellite cell-independent contribution to skeletal muscle fibers during adult
32 homeostasis.

33
34 **Abstract**

35 Adult skeletal muscle possesses remarkable regenerative capacity. This is attributed to
36 tissue-specific stem cells, satellite cells. Interstitial stromal cells also play critical roles in muscle,
37 and we have previously reported that *Hoxa11* and *Hoxd11*, expressed in the interstitial cells of
38 muscles that attach to the zeugopod (radius and ulna), are critical for the proper patterning and
39 development of these muscles during embryogenesis. Using a Hoxa11eGFP knock-in reporter,
40 we show that expression continues in a subset of muscle interstitial cells through adult stages.
41 Using *Hoxa11-CreERT2* mediated lineage reporting induced at adult stages, we observe lineage
42 initiation only in the interstitial cells of muscle, as expected. However, this Hoxa11-expressing
43 interstitial cell lineage progressively contributes to muscle fibers at postnatal and adult stages.
44 The contribution to these muscles at adult homeostasis significantly exceeds parallel *Pax7-*
45 *CreERT2* mediated lineage labeling performed in parallel. To confirm that interstitial cell nuclear
46 contents are contributed to muscle fibers, we additionally used the nuclear specific lineage
47 reporter, *ROSA-LSL-H2BmCherry* with *Hoxa11-CreERT2* and observe that Hoxa11-expressing
48 interstitial cells contribute their nuclei to myofibers. *Hox* lineage contribution is observed into
49 all four muscle sub-types over months of lineage labeling. At no point after Hoxa11-mediated
50 lineage induction do we observe lineage labeling into Pax7-expressing satellite cells. This adds
51 to a small but growing body of evidence that supports a satellite cell-independent source of
52 muscle tissue *in vivo*.

53

54

55 **Introduction**

56 Roles for *Hox* genes in the embryonic development of the skeletal system are well
57 established, with loss-of-function of *Hox* paralog groups leading to dramatic homeotic
58 transformations of the axial vertebrae, perturbed morphogenesis of the limb skeleton, and
59 disrupted organogenesis. In limb skeletal patterning, *Hox* paralog groups *Hox9 – Hox13* have
60 region specific function and loss of *Hoxa11* and *Hoxd11* gene function, dramatic mis-patterning
61 of the radius and ulna is observed (Davis and Capecchi, 1996; Fromental-Ramain et al., 1996a;
62 Fromental-Ramain et al., 1996b; Wellik and Capecchi, 2003). In compound *Hox11* mutants
63 where three of the four *Hoxa11* and *Hoxd11* alleles are absent, no skeletal phenotype results,
64 but patterning of the zeugopod-attached muscles and tendons is disrupted, supporting a direct
65 role for *Hox11* genes in muscle patterning (Swinehart et al., 2013).

66 *Hoxa11* gene expression initiates broadly in the lateral plate mesoderm of early developing
67 limb buds, but expression quickly localizes to the zeugopod region as it forms, and can be
68 observed throughout development in the stromal cells surrounding the developing cartilage
69 and bone, in the tendons, and in a continuous population of connective tissue/interstitial
70 stroma surrounding the zeugopod-attached myofibers (Swinehart et al., 2013). In this report,
71 we show that *Hoxa11*eGFP expression in zeugopod-attached muscle interstitial cells continues
72 throughout postnatal and adult life.

73 Limb skeletal muscle progenitors derive from the embryonic somites where muscle
74 precursors are marked by expression of *Pax3* and, later in development, *Pax7* (Chal and
75 Pourquié, 2017; Sefton and Kardon, 2019). *Pax3*⁺ progenitors delaminate from the somites and
76 migrate to the limb bud. These precursors undergo additional steps of myogenesis to generate
77 multinucleated myocytes (Chal and Pourquié, 2017; Nassari et al., 2017; Sefton and Kardon,
78 2019). After maturation, muscles retain significant plasticity with the ability to hypertrophy
79 with increased use and to repair in response to injury. Repair of skeletal muscle is known to rely
80 on satellite cells, stem cells set aside inside of the basal lamina of multi-nucleate muscle fibers
81 that are self-renewing and characterized by the expression of *Pax7* (Chal and Pourquié, 2017;
82 Lepper and Fan, 2010; Lepper et al., 2011; Pawlikowski et al., 2015; Yin et al., 2013). Ablation of

83 Pax7-expressing satellite cells leads to a profound deficit in the ability of skeletal muscle to
84 regenerate in response to injury (Lepper et al., 2011; Sambasivan et al., 2011). Pax7-mediated
85 lineage studies have demonstrated that satellite cells contribute to adult skeletal muscles at
86 homeostasis, however, ablation of satellite cells at adult stages, in the absence of injury, does
87 not lead to early sarcopenia and, surprisingly, skeletal muscle remains capable of hypertrophy
88 (Fry et al., 2015; Jackson et al., 2012; Keefe et al., 2015; McCarthy et al., 2011).

89 A heterogenous population of stromal cells, called interstitial cells, lie outside and surround
90 the basal lamina of the muscle fibers. Interstitial cells are critical for embryonic muscle
91 patterning; neither somite-derived muscle progenitors nor satellite cells possess intrinsic
92 muscle patterning information (Aoyama and Asamoto, 1988; Duprez, 2002; Lance-Jones, 1988;
93 Mathew et al., 2011; Michaud et al., 1997; Nassari et al., 2017). Multiple sub-populations of
94 interstitial cells have been defined, including pericytes, PW1+/Pax7- interstitial progenitor cells
95 (PICs), fibroblasts, fibroadipogenic progenitors (FAPs), and smooth muscle-mesenchymal cells
96 (SMMCs) (Giordani et al., 2019; Malecova and Puri, 2012; Mathew et al., 2011; Mierzejewski et
97 al., 2020a; Tedesco et al., 2017). How these interstitial cell populations are distinct from one
98 another is not fully understood, though there is at least some overlap between most of these
99 subsets (Malecova and Puri, 2012; Tedesco et al., 2017). Previous work has shown that
100 interstitial stromal cells support myofiber function and regeneration at adult stages, and can
101 impact satellite cell quiescence, activation, and migration (Heredia et al., 2013; Joe et al., 2010;
102 Kuswanto et al., 2016; Murphy et al., 2011; Nassari et al., 2017; Tatsumi et al., 2009; Thomas et
103 al., 2015; Tidball and Villalta, 2010; Uezumi et al., 2010).

104 A small but growing number of publications have reported that subsets of interstitial cells
105 possess myogenic potential, but the *in vivo* myogenic potential for these cells remains
106 controversial (Dellavalle et al., 2011; Doyle et al., 2011; Esteves de Lima et al., 2021; Giordani et
107 al., 2019; Liu et al., 2017; Mierzejewski et al., 2020b; Mitchell et al., 2010; Qu-Petersen et al.,
108 2002). Twist2-directed genetic lineage labeling from an interstitial cell sub-population
109 demonstrated direct contribution to adult skeletal muscle fibers *in vivo* (Liu et al., 2017).
110 Twist2-expressing cells were reported to contribute specifically to Type IIb/x myofibers at
111 homeostasis and following injury. Recently, it was reported that early lateral plate lineage cells

112 from a *Scx-Cre* reporter show contribution to muscle fibers and some of the satellite cell
113 population specifically at the myotendinous junction during embryogenesis (Esteves de Lima et
114 al., 2021).

115 In this study, we use our *Hoxa11eGFP* reporter and *Hoxa11-CreERT2* in combination with
116 *ROSA26-LSL-tdTomato* and *ROSA26-LSL-H2BmCherry* lineage reporters to examine *Hoxa11*
117 expression and the lineage contribution from Hox-expressing cells from embryonic to adult
118 stages (Blum et al., 2014; Madisen et al., 2010; Nelson et al., 2008; Pineault et al., 2019). We
119 demonstrate that *Hoxa11eGFP* expression is restricted to a sub-population of zeugopod-
120 attached, muscle interstitial cells at all stages of life. Flow cytometry and immunofluorescent
121 analyses show that *Hoxa11*-expressing cells are a non-hematopoietic, non-endothelial, non-
122 satellite cell stromal population with strong overlap with *Twist2* and partial overlap with *Tcf4*
123 and *PDGFR α* . *Hoxa11-CreERT2* lineage induction from any stage results in initiation of labeling
124 only in interstitial cells, as expected. Induction of lineage from E12.5 shows restriction of
125 reporter expression to only the muscle interstitial cells throughout the remainder of embryonic
126 development. However, at postnatal and adult stages, the *Hoxa11* lineage begins to show
127 contribution to myofibers. This contribution is progressive; reporter expression increases in
128 skeletal muscle fibers in the weeks after induction. In parallel experiments comparing *Hoxa11-*
129 *CreERT2* and *Pax7-CreERT2* to induce lineage labeling from the same *ROSA26-LSL-tdTomato*
130 reporter, *Hoxa11* lineage contribution is significantly higher than *Pax7*-expressing satellite cell
131 contribution to forelimb muscles during adult homeostasis. Intriguingly, the extent of *Hoxa11-*
132 mediated lineage labeling varies in a reproducible pattern in different muscle groups even
133 though *Hoxa11*-expressing interstitial cells are present in all zeugopod-attached muscles.
134 Contribution of *Hoxa11*-expressing interstitial cells to muscle fibers was further validated by
135 using a *Hoxa11-CreERT2;ROSA-LSL-H2BmCherry* reporter. Using this reporter, we demonstrate
136 that *Hoxa11*-expressing interstitial cells contribute their nuclei to myofibers. The *Hoxa11*
137 lineage does not mark *Pax7*-expressing satellite cells at any time point, supporting *Hox11-*
138 expressing cell contribution to myofibers that is independent from the satellite cell pool. Taken
139 together, these data support *Hoxa11*-expressing interstitial cells are a population of non-

140 satellite cell muscle progenitors *in vivo*. This report adds to the growing evidence for novel,
141 non-satellite cell sources of muscle progenitors *in vivo* in mammals.
142

143

144 **Results**

145 **Hoxa11eGFP expression is maintained in skeletal muscle interstitial cells throughout life.**

146 During development, Hoxa11eGFP expression in muscle is restricted to the zeugopod-
147 attached muscles, specifically in the non-endothelial interstitial stroma (Swinehart et al., 2013).
148 We examined expression at embryonic, postnatal, and adult stages and observed that
149 expression is maintained throughout life in zeugopod-attached skeletal muscle interstitial cells
150 (**Fig. 1A**). Using our previously validated *Hoxa11-CreERT2* to induce recombination of a *ROSA26-*
151 *Lox-STOP-Lox-tdTomato* lineage reporter (*Hoxa11iTom*; Madisen et al., 2010; Pineault et al.,
152 2019), we observe that 3 days after a single 5mg tamoxifen dose, *Hoxa11iTom* cells are
153 distributed throughout the interstitial cells of all forelimb muscles (**Fig 1B**). *Hoxa11iTom* lineage
154 is induced at approximately 90% efficiency at this tamoxifen dose and overlaps with
155 *Hoxa11eGFP* live reporter expression, validating our lineage reporter (**Fig 1C, Fig. S1**).
156 Additionally, *Hoxa11* expression in muscle is only in the interstitial cells (**Fig. S2**).

157

158 **Hoxa11eGFP-expressing cells are a non-hematopoietic, non-endothelial, non-satellite cell** 159 **sub-population of muscle interstitial cells.**

160 *Hoxa11eGFP*-expressing cells were assessed by flow cytometry to investigate how these
161 cells correlate with previously described populations of mononuclear cells present in skeletal
162 muscle. Live, mononucleated cells were enzymatically isolated from limb muscles attached to
163 the zeugopod (Liu et al., 2015), and cells were gated for CD45 and Ter119, to identify
164 hematopoietic cells. *Hoxa11GFP*-positive cells were essentially absent from the blood lineage,
165 as expected (**Fig 2A**). Non-hematopoietic cells were gated for CD31, an endothelial cell marker,
166 and we observed that *Hoxa11GFP*-positive cells were also largely absent from the endothelial
167 cell population (**Fig. 2B**). Of the non-hematopoietic, non-endothelial population, approximately
168 2% of remaining cells were *Hoxa11eGFP*-positive. Cells were further gated to identify satellite
169 cells, FAP cells and SMMCs (Smooth Muscle-Mesenchymal Cells) using the *Sca1*, *VCAM1* and
170 *ITGA7* cell surface markers (Giordani et al., 2019; Joe et al., 2010; Liu et al., 2013). While most
171 non-hematopoietic, non-endothelial cells are *Sca1*-negative (>75%), more than 50% of

172 Hoxa11GFP-positive cells segregated as Sca1-positive (**Fig. 2C**). Within this Sca1⁺/Hoxa11eGFP⁺
173 population, the majority (91%) of Hoxa11eGFP-positive cells are Itga7-negative, correlating with
174 previously identified FAPs (CD45⁺/CD31⁻/Sca1⁺/Itga7⁺, (Joe et al., 2010)). Among the non-
175 hematopoietic, non-endothelial, Hoxa11eGFP-positive cells that are Sca1-negative (just under
176 50% of total Hoxa11eGFP population), additional labeling with ITGA7 and VCAM1 showed that
177 the VCAM1⁺/Itga7⁺ satellite cell population contains essentially no Hoxa11eGFP⁺ cells (**Fig. 2E**).
178 A small fraction of the total Hoxa11eGFP⁺ cell population (~7%) segregated as CD45⁻/CD31-
179 /Sca1⁻/Itga7⁺/VCAM1⁻, markers reported recently to be a sub-population of interstitial SMMCs
180 that possess myogenic potential (Giordani et al., 2019).

181 We further characterized Hoxa11eGFP-expressing cells *in situ* by co-immunofluorescent
182 immunohistochemistry. Hoxa11eGFP expression is observed in interstitial cells outside the
183 basal lamina of myofibers and shows no overlap with satellite cells based on Pax7 and laminin
184 immunostaining (**Fig. 2F**). The transcription factor, Twist2, is expressed in interstitial cells that
185 possess previously reported myogenic potential (Li et al., 2019; Liu et al., 2017); we observe
186 that most Hoxa11eGFP-expressing cells also express Twist2, though the two populations are
187 not completely overlapping (**Fig. 2G**). Within the interstitial population, Hoxa11eGFP also shows
188 partial overlap with PDGFR α , a marker used to identify FAPs, and low overlap with Tcf4, a
189 connective tissue fibroblast marker (Joe et al., 2010; Mathew et al., 2011; Murphy et al., 2011;
190 Uezumi et al., 2010; Uezumi et al., 2011). Using our *Hoxa11* lineage reporter (Hoxa11iTom) we
191 further demonstrate that, *Hoxa11* lineage labeled cells (3-days after tamoxifen treatment) do
192 not colocalize with PECAM/CD31⁺ endothelial cells (**Fig. 2J**). These results corroborate and
193 extend flow cytometry analyses and demonstrate that Hoxa11eGFP is expressed in a sub-
194 population of muscle interstitial cells.

195

196 ***Hoxa11* lineage in muscle tissue remains restricted to interstitial cells during embryonic**
197 **stages but begins contributing to myofibers at postnatal stages.**

198 We next sought to examine the lineage of the Hoxa11-expressing population. To assess
199 embryonic lineage, pregnant dams were dosed with tamoxifen at E12.5 and resulting

200 *Hoxa11*^{CreERT2/+}; *ROSA*^{LSL-tdTomato/+} embryos were collected at E18.5. Hoxa11iTom expression is

201 observed exclusively in the interstitial and connective tissue cells of developing muscles (**Fig**
202 **3A**).

203 Postnatal lineage was examined by dosing *Hoxa11*^{CreERT2/+}; *ROSA*^{LSL-tdTomato/+} animals with
204 tamoxifen on postnatal day 3 (P3) and collecting them at P7, P14, and P28 (**Fig 3B**). Whole
205 forelimb cross-sections and higher magnification images show tdTomato expression within
206 tendon, bone, and muscle at all time points. *Hoxa11*iTom is expressed throughout the
207 zeugopod forelimb in muscle interstitial cells at P7. At this time point, very low levels of
208 tdTomato expression can be observed in a small number myofibers. Images of P7, P14, and P28
209 taken at the same exposure show increasing number and intensity of tdTomato+ myofibers
210 with time after induction.

211 A recent report identified an unexpected contribution to the myogenic lineage from
212 embryonic lateral plate mesoderm using both quail-chick chimeras and using a *Scleraxis-Cre*
213 allele and reported *Scx-Cre*-mediated contribution to the embryonic myogenic lineage at or
214 near the myotendinous junction (Esteves de Lima et al., 2021). We observe no such localization
215 to the myotendinous junction region at embryonic or adult stages (**Fig. S3**). Together our data
216 supports a *Hoxa11* lineage that is restricted to the muscle interstitium throughout embryonic
217 stages but begins to progressively contribute to myofibers during the postnatal period.

218

219 ***Hoxa11*-expressing cells make progressive contribution to adult skeletal myofibers at**
220 **homeostasis to a greater extent than *Pax7* lineage-induced satellite cells.**

221 To assess *Hoxa11* lineage behavior at adult stages, *Hoxa11*^{CreERT2/+}; *ROSA*^{LSL-tdTomato/+} animals
222 were dosed with 5 mg tamoxifen at 8 weeks of age and analyzed at 2-, 4-, 7-, 14-, and 56-days
223 after tamoxifen induction (**Fig. 4A**). At 4 days post-induction, there is extensive lineage labeling
224 of muscle interstitial cells and only faint tdTomato signal in a few muscle fibers. At continuing
225 time points through 8 weeks post-induction, lineage contribution to muscle fibers progressively
226 increases as seen in whole forelimb cross-sections and magnifications of three different
227 muscles (**Fig. 4B**). Continual, progressive, and more extensive lineage labeling is observed at
228 later stages (**Fig. S4**). The extent of lineage labeling into each muscle group varies, but with high
229 reproducibility between animals. In *Hoxa11*iTom animals at 8 weeks after induction, the

230 Extensor Carpi Ulnaris (ECU) shows 95.2% +/- 2.9 tdTomato-positive fibers. The Flexor
231 Digitorum Profundus (FDP) shows 51.2% +/- 6.9 tdTomato-positive muscle fibers, and the Flexor
232 Digitorum Sublimis (FDS) has 20.5% +/- 4.9 tdTomato-positive fibers. Despite differential
233 lineage labeling into muscle groups, Hoxa11iTom-labeled interstitial cells are observed
234 relatively uniformly throughout forelimb muscle tissue (**Fig. 1B; Fig S2**). Hindlimbs from these
235 animals were also examined and the extent of lineage contribution to myofibers is comparable
236 to the forelimb (**Fig. S5**).

237 Parallel experiments were performed with the same reagents using *Pax7^{CreERT2/+}; ROSA^{LSL-}*
238 *tdTomato/+* mice (Pax7iTom) (Murphy et al., 2011) to compare Hoxa11 lineage contribution to
239 satellite cell contribution at homeostasis. Animals were given the same tamoxifen treatment
240 and this resulted in ~90% efficient recombination in the *Pax7^{CreERT2/+}; ROSA^{LSL-tdTomato/+}* animals
241 as well (**Fig. S1**). The observed lineage contribution of Pax7-expressing satellite cells was
242 significantly less than from Hoxa11-expressing cells (**Fig. 4B-D**). Of note, Pax7 lineage
243 contribution was more evenly distributed throughout the muscle groups, with low but
244 consistent increases in the amount of lineage-labeled myofibers over time, consistent with
245 findings reported previously in the hindlimb (Keefe et al., 2015; Pawlikowski et al., 2015). In
246 examining the same three muscle groups, Pax7iTom contribution is 15.7% +/- 3.3 in the ECU,
247 21.5% +/- 3.1 in the FDP, and 16.4% +/- 2.1 in the FDS. High-magnification images of the ECU,
248 FDP, and FDS muscle from Pax7iTom animals are shown in **Fig. S6**. Comparative quantification
249 of lineage-positive myofibers of the FDP, ECU and FDS from both Hoxa11iTom and Pax7iTom
250 animals at 8 weeks after induction shows Hoxa11iTom contribution is significantly higher in
251 both the FDP and ECU muscles (**Fig. 4D**).

252 Our results show many similarities to those reported for Twist2-expressing interstitial cells
253 (Liu et al., 2017) and, intriguingly, Hoxa11eGFP and Twist2 expression are highly overlapping.
254 We sought next to interrogate whether this cellular lineage behavior occurs from other
255 populations of muscle interstitial cells. PDGFR α is a more broadly expressed interstitial cell
256 marker, so we utilized a *PDGFR α -CreERT2* and the *ROSA-LSL-tdTomato* reporter (PDGFR α iTom)
257 to investigate the lineage contribution to myofibers (Rivers et al., 2008). Using this model, we
258 do not observe lineage labeling into myofibers, even 10 weeks after adult induction (**Fig. 4E**).

259 Of note, there is previously reported evidence that tdTomato mRNA can be packaged in
260 extracellular vesicles that enter the myofiber, resulting in fusion-independent lineage reporter
261 expression within muscle fibers (Murach et al., 2020). Close examination of the PDGFR α iTom
262 shows a small number of myofibers (~5 in a whole forelimb cross-section) with low levels of red
263 fluorescence, perhaps indicative of this type of non-specific labeling (**Fig. 4E**). However, the
264 relative lack of myofiber lineage labeling in the PDGFR α iTom animals supports that lineage
265 contribution in the Hoxa11iTom model does not result from leaky expression or fusion of
266 cytoplasmic vesicles.

267

268 ***Hoxa11* lineage demonstrates nuclear contribution to myofibers**

269 To provide additional evidence that the observed Hoxa11iTom lineage represents
270 contribution of interstitial cells to myofibers and is not due to transport of tdTomato+
271 cytoplasm or tdTomato mRNA into muscle fibers, we generated a *Hoxa11*-dependent nuclear
272 lineage reporter, by crossing our *Hoxa11-CreERT2* line with *ROSA-LSL-H2BmCherry* (Blum et al.,
273 2014). Resulting *Hoxa11^{CreERT2/+}; ROSA^{LSL-H2B-mCherry/+}* (Hoxa11iH2BmCherry) animals were given
274 5mg tamoxifen at 6 weeks of age and collected at 4 days and 2 weeks after induction (**Fig 5A**).
275 H2BmCherry-labeled myonuclei are clearly observed in muscle interstitial cells 4 days after
276 tamoxifen induction (**Fig 5B**). By 2 weeks after lineage induction, Hoxa11iH2BmCherry+ nuclei
277 can be additionally visualized within myofibers under the basal lamina (**Fig. 5C**).
278 Hoxa11iH2BmCherry-positive nuclei were confirmed with DAPI staining (Fig. S7). These
279 experiments provide strong support for *Hoxa11*-expressing interstitial cells contributing full
280 cellular contents, including their nuclei, to muscle fibers *in vivo*.

281

282 ***Hoxa11* lineage contributes to all muscle fiber types.**

283 Previous publications have reported that *Twist2*-mediated contribution to muscle exhibits
284 fiber-type specificity, contributing to only Type IIb/x myofibers (Li et al., 2019; Liu et al., 2017).
285 Of note, these experiments were conducted on animals that were lineage labeled for up to four
286 months. Observation of the Hoxa11iTom lineage in the hindlimb at 3 weeks following adult
287 induction supports this specificity as almost no lineage labeling is observed in the soleus, which

288 is comprised of mainly Type 1 myofibers while fairly extensive labeling is observed in the
289 adjacent gastrocnemius, which is mainly Type IIb and IIx (**Fig. S5**)(Burkholder et al., 1994).
290 However, upon evaluation of myofiber type specificity in Hoxa11iTom lineage at 8 months after
291 induction of the reporter (10 months of age), Hoxa11 lineage contributes to all four muscle
292 types, Type I, IIa, IIb, and IIx, is observed (**Fig 6A-D**).

293

294 **Satellite cells are not lineage labeled by the *Hoxa11* lineage reporters**

295 To determine whether Hoxa11-mediated lineage labeling results in reporter expression in
296 satellite cells, we carefully examined co-expression of Pax7 and Hoxa11iTom in both the
297 forelimb and the hindlimb of Hox11iTom animals. In the forelimb at 2 weeks after lineage
298 induction, the ECU, FDP, and FDS were assessed for overlap of Hox11iTom and Pax7; we
299 observed 0 instances of co-expression of Pax7 and Hoxa11iTom among a total of 1,048
300 individual, DAPI-stained cells analyzed (**Fig. 7A-D**). We further assessed Hoxa11 lineage and
301 Pax7 antibody staining 8 weeks after lineage induction and again found no tdTomato+ satellite
302 cells from 311 cells counted (**Fig. S8**). In the hindlimb, we analyzed three muscle groups, the
303 Gastrocnemius/Plantaris, Soleus, and Tibialis Anterior for possible Hoxa11iTom and Pax7 co-
304 expression. Consistent with data collected for the forelimb, no overlap of Hoxa11 lineage and
305 Pax7 was observed out of 695 cells analyzed (**Fig. 7E-G**). Using our nuclear specific reporter
306 (Hoxa11-H2BmCherry), we assessed whether any Pax7+ cells were H2BmCherry+. We observed
307 zero Pax7+/mCherry+ cells 2 weeks after reporter induction (**Fig. 7H**) These results indicate
308 Hoxa11-expressing cells do not contribute to or non-specifically label the satellite cell
309 population.

310

311

312 **Discussion**

313 Uncovering the cell types that are responsible for muscle maintenance and growth is crucial
314 to understanding skeletal muscle's dynamic nature and its remarkable regenerative capacity. In
315 this study we show definitive interstitial cell contribution to myofibers *in vivo* beginning at
316 postnatal stages through genetic lineage labeling of Hoxa11-expressing interstitial fibroblasts.
317 The Hoxa11 lineage initiates only in interstitial cells and remains solely in this population
318 through embryonic development, but then contributes progressively to skeletal muscle fibers at
319 postnatal and adult stages. Hoxa11 is not expressed in the satellite cell population. Further, we
320 show that Hoxa11-expressing interstitial cells do not lineage label into satellite cells after
321 lineage induction, indicating interstitial cell contribution is not mediated through the satellite
322 cell pool. Thus, Hoxa11-expressing cells are a unique set of progenitors.

323 There has been mounting evidence that some skeletal muscle interstitial cells have
324 myogenic potential. Studies at postnatal time points have indicated that PICs can contribute to
325 muscle fibers upon transplantation and can differentiate into myocytes *in vitro*, however, their
326 endogenous biological role remains unclear (Mitchell et al., 2010). Using a *Alkaline*
327 *Phosphatase-CreERT2*, authors report that pericytes contribute to the satellite cell pool and to
328 muscle fibers, but after the postnatal stages, researchers observed very few lineage labeled
329 fibers, even following cardiotoxin injury (Dellavalle et al., 2011). Twist2-directed genetic
330 lineage labeling of interstitial cells previously reported non-satellite cell contribution to
331 myofibers at adult stages *in vivo* with many similarities to the findings in this report. The strong
332 overlap between Twist2 and Hoxa11eGFP expression suggests these two transcription factors
333 mark a subset of interstitial cells that are relevant for this activity *in vivo*. The absence of
334 lineage labeling into muscle fibers using *PDGFR α -CreERT2*, which is a broader, less specific
335 marker of interstitial cells, further supports the notion that only of a unique subset of
336 interstitial cells is capable of contributing to myofibers *in vivo*.

337 Another fibroblast population with potential myogenic activity was recently reported
338 using single cell RNA-sequencing in conjunction with mass cytometry and his new population
339 was named smooth muscle mesenchymal cells (SMMCs). These cells are ITGA7+VCAM1-, thus

340 distinct from satellite cells which are VCAM1+ (Giordani et al., 2019). SMMCs were reported to
341 have myogenic capacity *in vitro* and to contribute to myofibers upon transplantation into
342 injured muscle. Our flow cytometry data shows relatively few (~7%) Hoxa11eGFP+ cells in this
343 ITGA7+VCAM1- population, however, more rigorous genetic and transcriptomic comparisons
344 will serve to clarify the relationship between these cells.

345 The wealth of literature and decades of research on satellite cells and their critical role
346 as myofiber stem cells puts an exceedingly high burden of proof on new biology that suggests
347 there may be an additional, interstitial cell progenitor pool important during mature muscle
348 homeostasis. Strong genetic evidence of cellular behavior *in vivo* was provided by the reports
349 that Twist2-expressing interstitial cells contribute to muscle fibers at homeostasis (Li et al.,
350 2019; Liu et al., 2017). In this report, we show very similar ROSA-tdTomato lineage contribution
351 from an independently generated, distinct genetic locus of another transcription factor
352 (Hoxa11) that is expressed in a similar subset of muscle interstitial cells. There is reported
353 evidence of non-specific cytoplasmic transport of fluorescent reporter mRNAs and proteins to
354 other cells (Murach et al., 2020). To address this potential caveat, we carried out an additional
355 line of genetic experiments using the ROSA-LSL-H2BmCherry lineage reporter. Using this
356 nuclear localized lineage reporter, we show initial labeling in interstitial cell nuclei, but
357 relatively rapid and distinct contribution of H2BmCherry-labeled nuclei into muscle fibers.
358 Further, we show that *PDGFR α -CreERT2*-induced ROSA-tdTomato lineage labeling, which
359 results in extensive labeling of a broader population of interstitial cells and connective tissue,
360 does not lead to contribution to muscle fibers even 10 weeks after induction (with the
361 exception of a few faint red muscle fibers that may indeed be reflective of cytoplasmic content
362 sharing). Thus, the collective evidence strongly supports the specificity and uniqueness of a
363 subset of interstitial cells with myogenic potential *in vivo*.

364 Further investigation is needed to understand more about this unique and important
365 subset of interstitial cell myofiber progenitors, including the degree of stemness they possess,
366 their contribution to myofibers during aging, exercise, and in response to injury, and their
367 behavior *in vitro* and in transplantation experiments. This understudied population and its

368 ability to contribute to muscle fibers at homeostasis *in vivo* has exciting potential to lead to new
369 therapies for those suffering from myopathies and muscular dystrophies.
370

371

372 Methods and Materials

373 Mouse models

374 Generation of mouse models *Hoxa11^{eGFP}* (Nelson et al., 2008), *Hoxa11-CreERT2* (Pineault
375 et al., 2019), *Pax7-CreERT2* (Murphy et al., 2011), *PDGFR α -CreERT2* (Rivers et al., 2008), and
376 *ROSA-LSL-H2B-mCherry* have been previously described. The *ROSA26-CAG-loxP-STOP-loxP-*
377 *tdTomato* (JAX stock no. 007909, Madisen et al., 2010) was purchased from The Jackson
378 Laboratory. Creation of *Hoxa11^{iTom}* mice was achieved by crossing *Hoxa11^{CreERT2/+}* males with
379 *Hoxa11^{eGFP/+}*; *ROSA^{LSL-tdTomato/LSL-tdTomato}* females. Generation *Pax7^{iTom}* mice was achieved by
380 crossing *Pax7^{CreERT2/+}* males with *ROSA^{LSL-tdTomato/LSL-tdTomato}* females. All mouse colonies were
381 maintained on a mixed genetic background. Both male and female mice were used in all
382 experiments (and all control and mutant pairs were sex-matched). Animals used in this study
383 were euthanized by CO₂ followed by cervical dislocation. All procedures described are in
384 compliance with protocols approved by the University of Wisconsin-Madison and the University
385 of Michigan Committee on Animal Care and Use Committees.

386

387 Tamoxifen treatment

388 Adult mice were given a single intraperitoneal (IP) injection of 5mg tamoxifen (Sigma T5648)
389 dissolved in corn oil at 8 weeks of age and collected at indicated time points. Embryonic
390 induction was achieved by mating *Hoxa11^{CreERT2/+}* males to *Hoxa11^{eGFP/+}*; *ROSA^{LSL-tdTomato/LSL-}*
391 *tdTomato* females and presence of the vaginal plug was checked each morning. Pregnant dams
392 were given 2mg tamoxifen and 1mg/mL progesterone dissolved in corn oil via intraperitoneal
393 injection at indicated embryonic time points (Pineault et al., 2019). Postnatal animals were
394 given 0.25mg of tamoxifen dissolved in corn oil via intragastric injection on postnatal day 3.

395

396 Tissue Preparation

397 Left and right zeugopods were collected. Skin and soft tissues were removed from the
398 region and the zeugopod muscles and skeleton was isolated. Muscles were either carefully
399 dissected off the bone or muscle was left attached to the bone. Dissection was done in PBS.

400 Muscle groups and intact limbs were fixed in 4% paraformaldehyde (PFA, Sigma) in PBS shaking
401 at 4 °C for 1-3 days. Intact limbs were decalcified in 14% ethylenediaminetetraacetic acid (EDTA,
402 EMD Millipore) for 3-5 days (postnatal animals) or 6-7 days (adults) at 4 °C. Samples were
403 cryoprotected in 30% sucrose in PBS overnight before embedding in OCT compound (Fisher, cat
404 no. 4585). Tissue was stored a -80 °C. Cryosections of 10-14 µm were analyzed by IF.

405

406 Immunohistochemistry

407 Sections were rehydrated with PBS. In some cases, antigen retrieval was performed by
408 heating slides in a citrate buffer for 10-30 min and blocked with TNB buffer (Perkin Emler
409 FP1020). Sections were incubated in primary antibodies overnight at 4 °C and then incubated in
410 secondary antibodies for 2 hours at room temperature and counterstained with DAPI for
411 nuclear visualization. Antibody information is provided in supplementary information (**Table**
412 **S1**). tdTomato and mCherry were visualized directly with no antibody staining. Slides were
413 mounted with ProLong Gold antifade reagent (Invitrogen, cat no. P36930). Staining using
414 mouse monoclonal antibodies utilized a mouse-on-mouse immunodetection kit (Vector Labs,
415 cat no. BMK-2202) according to vendor instructions.

416 Imaging was performed on the Nikon eclipse Ti, Keyence BZ-X800, and Leica SP8 3X STED
417 Confocal. Image editing was preformed using ImageJ and Photoshop, and larger images were
418 stitched together (when necessary) on photoshop or by the Keyence BZ-X800 analyzer.

419

420 Quantification

421 For calculation of percent positive tdTomato myofibers from Hoxa11iTom and Pax7iTom
422 mice, multiple representative fields of view, from the ECU, FDP, and FDS muscles collected 8
423 weeks after Cre induction, were compiled. A blinded participant counted the total number of
424 myofibers in the field of view and the total number of tdTomato positive. Percent of tdTomato
425 positive myofibers was calculated; data was transferred to GraphPad Prism9 where statistical
426 analysis for significance, between Hoxa11iTom and Pax7iTom ECU, FDP, and FDS muscles, and
427 standard error was performed. To assess overlay of Hoxa11 lineage labeled cells with Pax7,
428 tissue from Hoxa11iTom mice was collected at 2 weeks and 8 weeks post induction; sections

429 were stained using an anti-Pax7 antibody (DSHB). 3-5 fields of view from each animal (n=3 for
430 both forelimb and hindlimb analyses) were used; Pax7 and Hoxa11iTom cells were identified,
431 counted, and profiled into three groups: Hoxa11iTom+/Pax7-, Hoxa11iTom-/Pax7+, or
432 Hoxa11iTom+/Pax7+. Statistical analyses were carried out by an unpaired Student's t-test
433 (GraphPad Prism9).

434

435 Flow Cytometry

436 To isolate mononuclear populations from muscle, zeugopod-attaching muscles were
437 removed from the forelimb and hindlimb. Dissected muscles were chopped into smaller pieces
438 followed by digestion in 700 U/mL collagenase type II (Gibco, cat no. 17101-015) at 37°C for 1
439 hour. After spin and trituration steps muscles underwent a second digestion in 100 U/mL
440 collagenase type II and 1.1 U/mL dispase (Gibco, cat no. 17105-041) for 30 min at 37°C. Cells
441 were washed, triturated, spun, and filtered through a 40-micron cell strainer before being
442 placed in 1xPBS with 2% FBS (Gibco). Flow cytometry experiments were carried out on the
443 ThermoFisher Attune NxT Flow Cytometer BRYV. Markers and antibody information is provided
444 in supplemental information (**Table S1**). Analysis was preformed using FloJo.

445

446 Acknowledgments

447 We sincerely thank and are grateful for experiments performed by Anna P. Miller, PhD and
448 assistance provided by Alex Hurley. We'd like to thank Gabrielle Kardon, PhD for providing the
449 Pax7-CreERT2 mouse model and Barak Blum, PhD for providing the ROSA-H2B-mCherry mouse
450 model, this work would not have been possible without those animals. Further, this work was
451 supported by AR072511 (DMW) and the Flow Cytometry Laboratory at University of Wisconsin-
452 Madison and their funding source CA014520.

453

454

455 **Figure Legends**

456

457 **Figure 1. Hoxa11 expression is maintained in skeletal muscle interstitial cells throughout life.**

458 (A) Hoxa11eGFP real-time reporter shows expression (green) at E18.5 and P7 surrounding
459 muscle fibers (MY32, white). At 8 weeks of age, Hoxa11eGFP (green, yellow arrows) is
460 expressed in the interstitium visualized with WGA (white). (B) High magnification images from a
461 whole forelimb cross section show tdTomato expression (Hoxa11iTom, red) in the interstitium
462 throughout forelimb muscles. (C) Hoxa11 lineage reporter (Hoxa11iTom, red) overlaps with
463 real-time reporter Hoxa11eGFP (green, white arrowheads) in interstitial cells 3 days post-
464 tamoxifen.

465

466 **Figure 2. Hoxa11eGFP-positive cells are a subset of interstitial cells.** Flow cytometric analyses

467 of mononucleated live cells from zeugopod muscles of 14-week-old mice stained with CD45,
468 TER119, CD31, Sca1, Itga7 and VCAM1. After sorting by forward scatter, side scatter and using
469 DAPI for exclusion of dead cells, Hoxa11eGFP+ cells sort as non-hematopoietic (CD45- and
470 TER119-negative), (A), and non-endothelial (CD31-negative), (B). (C) Within the non-
471 hematopoietic, non-endothelial population, Hoxa11eGFP+ cells sort as 51% Sca1-positive and
472 49% Sca1-negative cells. (D) The majority of Hoxa11eGFP+/Sca1+ cells are Itga7-negative
473 (FAPs). (E) The Hoxa11eGFP+/Sca1- population is negative for VCAM1, and Hoxa11eGFP+/Sca1-
474 cells do not sort with the Itga7+/VCAM+ satellite cells. Approximately 8% of the
475 Hoxa11eGFP+/Sca1- cells are Itga7+/VCAM-, a marker combination used to identify SMMCs.
476 Hoxa11eGFP+ cells are represented as green dots on top of gray-scale density plots of non-GFP
477 labeled cells. Forelimb ventral muscle sections of 8–10-week-old animals were immunostained
478 for GFP, Pax7 and WGA (F); GFP, Twist2 and WGA (G); GFP, PDGFR α and WGA (H); GFP, Tcf4
479 and WGA (I). (F) Hox11eGFP+ (arrows) cells do not overlap with Pax7+ satellite cells
480 (arrowheads). Arrows (white) in G-J indicate double positive cells. Arrowheads (yellow) in G-J
481 indicate Hox11eGFP+ cells. (J) Hoxa11 lineage positive cells (Hoxa11iTom, arrows), 4-days post
482 tamoxifen, do not colocalize with PECAM/CD31 (arrowheads). Scale bars, 50 μ m.

483

484 **Figure 3. Embryonic *Hoxa11* lineage is exclusively interstitial; postnatal lineage begins to**
485 **contribute to myofibers.** At E12.5 the pregnant dams were dosed with 5mg Tamoxifen by
486 intraperitoneal injection and embryos were collected at E18.5. (A) Representative cross-section
487 of E18.5 forelimb stained for My32 (white) with *Hoxa11*iTom (red) visible in connective tissue
488 and bone; nuclear staining shown with DAPI (blue). High magnification of E18.5 forelimb muscle
489 shows tdTomato signal does not overlap with My32. (B) At postnatal day 3 *Hoxa11*^{CreERT2/+};
490 *ROSA*^{LSL-tdTom/+} mice were given 0.25mg Tamoxifen by intragastric injection and collected at P7,
491 P14, and P28. (C) Full forelimb cross sections show tdTom (*Hoxa11*iTom) expression throughout
492 forelimb tissues and high magnification images show clear tdTom expression in myofibers at
493 P14 and P28. Inset of P7 muscle shows some faint tdTom⁺ myofibers when imaged at a higher
494 exposure. Scale bars, 100µm

496 **Figure 4. *Hoxa11*-expressing skeletal muscle interstitial cells progressively contribute to**
497 **myofibers in the adult mouse forelimb.** (A) *Hoxa11*^{CreERT2/eGFP};*ROSA*^{LSL-TdTom/+} (*Hoxa11*iTom)
498 mice were given a single intraperitoneal injection of 5 mg tamoxifen at 8 weeks of age and
499 collected at 2 days, 4 days, 1 week, 2 weeks, and 8 weeks after tamoxifen induction. (B) Whole
500 forelimb cross-sections were collected at time points indicated. Images of Extensor Carpi
501 Ulnaris (ECU), Flexor Digitorum Profundus (FDP), and Flexor Digitorum Sublimis (FDS) muscles
502 from *Hoxa11*iTom muscle show increasing number of tdTomato expressing myofibers over
503 time. (C) Full forelimb cross-sections from *Pax7*^{CreERT2/+};*ROSA*^{LSL-TdTom/+} (*Pax7*iTom) animals
504 shows fewer tdTomato positive myofibers compared to *Hoxa11*iTom animals at the same time
505 points. (D) Quantification of percentage tdTomato-positive myofibers from ECU, FDS, and FDP
506 muscles from *Hoxa11*iTom and *Pax7*iTom animals 8 weeks post-induction (n=3 animals, 2-5
507 fields of view per muscle group analyzed). Statistics by Student's t-test. ns, not significant.
508 White dashed line marks borders of muscles shown in B and quantified in D, position of radius
509 and ulna marked by R and U, respectively. (E) *PDGFRα*^{CreERT2/+};*ROSA*^{LSL-tdTomato/+} (*PDGFRα*iTom)
510 animals were treated with 5 mg tamoxifen at 8 weeks of age and collected 10 weeks later.
511 Whole cross section of the forelimb shows tdTomato expression in connective tissues, bone
512 tissue, tendons, and the muscle interstitium. High magnification images of skeletal muscle

513 shows PDGFR α iTom expression in the muscle interstitium. A few myofibers were noticed to
514 have low tdTomato expression marked by asterisks (*).

515

516 **Figure 5. Hoxa11-expressing interstitial cells contribute their nuclei to myofibers. (A)**

517 *Hoxa11*^{CreERT2/+}; *ROSA*^{LSL-H2BmCherry/+} mice were given 5mg of tamoxifen at 6 weeks of age and
518 collected 4 days and 2 weeks after dosing. (B) Top, left image shows a cross section of the
519 forelimb of an adult mouse 4-days post-tamoxifen dosing. The larger, bottom image is a higher
520 magnification image of the tissue in the white dashed box. The three top, right images are high
521 resolution pictures of interstitial or myofiber nuclei from the bottom panel. (C) Top, left image
522 shows a cross section of the forelimb of an adult mouse 2-weeks post-tamoxifen dosing. The
523 larger, bottom image is a higher magnification image of the tissue in the white dashed box. The
524 three top, right images are high resolution pictures of interstitial or myofiber nuclei from the
525 bottom panel. Yellow arrowheads point to H2BmCherry labeled interstitial cell nuclei; white
526 arrows point to H2BmCherry labeled myonuclei in B and C.

527

528 **Figure 6. Hoxa11 lineage contributes to Type I, Type IIa, Type IIb, and Type IIx myofibers. (A)**

529 Mice were treated with tamoxifen at 8-weeks of age and collected at 10 months of age. (B-D)
530 *Hoxa11* lineage labeled myofibers are identified by tdTomato signal (*Hoxa11*iTom). Myofiber
531 sub-types were identified by immunofluorescent staining with anti-myosin (Slow), anti-SC-71,
532 and anti-BF-F3 (additional antibody details are available in Supplemental Table 1). (E) Type IIx
533 fibers were identified by the absence of combined markers. Fibers shown are from the
534 Gastrocnemius/Plantaris muscles. Lineage labeling is observed in all myofiber sub-types (white
535 arrows). Scale bar = 100 μ m.

536

537 **Figure 7. Pax7-expressing satellite cells are not lineage labeled by Hoxa11 lineage.**

538 *Hoxa11*^{CreERT2/+}; *ROSA*^{LSL-tdTom/+} mice given a single 5mg dose of tamoxifen by intraperitoneal
539 injection at 8 or 12 weeks of age were collected 2-weeks later. (A) Pax7 cells (cyan, yellow
540 arrows) are visualized under the basal lamina (white) with zero incidences of *Hoxa11* lineage
541 labeling (red) of Pax7-expressing cells in forelimb skeletal muscle at 2 weeks post-induction. (B-

542 **G).** The number of Hoxa11iTom and Pax7 single- or double-positive cells were quantified in the
543 Extensor Carpi Ulnaris (ECU), Flexor Digitorum Profundus (FDP), and Flexor Digitorum Sublimis
544 (FDS) muscles of the forelimb and the Gastrocnemius/Plantaris (G/P), Soleus (SL), and Tibialis
545 Anterior (TA) muscles of the hindlimb. **(H)** *Hoxa11^{CreERT2/+}; ROSA^{LSL-H2B-mCherry/+}* animals were
546 given a single 5mg dose of tamoxifen by intraperitoneal injection at 6 weeks of age and
547 immunostained for Pax7+ satellite cells 2 weeks after dosing; no overlap of
548 Hoxa11iH2BmCherry and Pax7 were observed.
549

550
551
552
553
554
555
556
557
558
559
560
561
562
563
564
565
566
567
568
569
570
571
572
573
574
575
576
577
578
579
580
581
582
583
584
585
586
587
588
589
590

References

- Aoyama, H. and Asamoto, K.** (1988). Determination of somite cells: independence of cell differentiation and morphogenesis. *Development* **104**, 15-28.
- Blum, B., Roose, A. N., Barrandon, O., Maehr, R., Arvanites, A. C., Davidow, L. S., Davis, J. C., Peterson, Q. P., Rubin, L. L. and Melton, D. A.** (2014). Reversal of β cell de-differentiation by a small molecule inhibitor of the TGF β pathway. *eLife* **3**, e02809-e02809.
- Burkholder, T. J., Fingado, B., Baron, S. and Lieber, R. L.** (1994). Relationship between muscle fiber types and sizes and muscle architectural properties in the mouse hindlimb. *J Morphol* **221**, 177-190.
- Chal, J. and Pourquié, O.** (2017). Making muscle: skeletal myogenesis in vivo and in vitro. *Development* **144**, 2104-2122.
- Davis, A. P. and Capecchi, M. R.** (1996). A mutational analysis of the 5' HoxD genes: dissection of genetic interactions during limb development in the mouse. *Development* **122**, 1175-1185.
- Dellavalle, A., Maroli, G., Covarello, D., Azzoni, E., Innocenzi, A., Perani, L., Antonini, S., Sambasivan, R., Brunelli, S., Tajbakhsh, S., et al.** (2011). Pericytes resident in postnatal skeletal muscle differentiate into muscle fibres and generate satellite cells. *Nat Commun* **2**, 499.
- Doyle, M. J., Zhou, S., Tanaka, K. K., Piscconti, A., Farina, N. H., Sorrentino, B. P. and Olwin, B. B.** (2011). Abcg2 labels multiple cell types in skeletal muscle and participates in muscle regeneration. *J Cell Biol* **195**, 147-163.
- Duprez, D.** (2002). Signals regulating muscle formation in the limb during embryonic development. *Int J Dev Biol* **46**, 915-925.
- Esteves de Lima, J., Blavet, C., Bonnin, M.-A., Hirsinger, E., Comai, G., Yvernogeu, L., Delfini, M.-C., Bellenger, L., Mella, S., Nassari, S., et al.** (2021). Unexpected contribution of fibroblasts to muscle lineage as a mechanism for limb muscle patterning. *Nature Communications* **12**, 3851.
- Fromental-Ramain, C., Warot, X., Lakkaraju, S., Favier, B., Haack, H., Birling, C., Dierich, A., Dollé, P. and Chambon, P.** (1996a). Specific and redundant functions of the paralogous Hoxa-9 and Hoxd-9 genes in forelimb and axial skeleton patterning. *Development* **122**, 461-472.
- Fromental-Ramain, C., Warot, X., Messadecq, N., LeMeur, M., Dollé, P. and Chambon, P.** (1996b). Hoxa-13 and Hoxd-13 play a crucial role in the patterning of the limb autopod. *Development* **122**, 2997-3011.
- Fry, C. S., Lee, J. D., Mula, J., Kirby, T. J., Jackson, J. R., Liu, F., Yang, L., Mendias, C. L., Dupont-Versteegden, E. E., McCarthy, J. J., et al.** (2015). Inducible depletion of satellite cells in adult, sedentary mice impairs muscle regenerative capacity without affecting sarcopenia. *Nat Med* **21**, 76-80.

- 591 **Giordani, L., He, G. J., Negroni, E., Sakai, H., Law, J. Y. C., Siu, M. M., Wan, R., Corneau, A.,**
592 **Tajbakhsh, S., Cheung, T. H., et al.** (2019). High-Dimensional Single-Cell Cartography
593 Reveals Novel Skeletal Muscle-Resident Cell Populations. *Mol Cell* **74**, 609-621.e606.
- 594 **Heredia, J. E., Mukundan, L., Chen, F. M., Mueller, A. A., Deo, R. C., Locksley, R. M., Rando, T.**
595 **A. and Chawla, A.** (2013). Type 2 innate signals stimulate fibro/adipogenic progenitors
596 to facilitate muscle regeneration. *Cell* **153**, 376-388.
- 597 **Jackson, J. R., Mula, J., Kirby, T. J., Fry, C. S., Lee, J. D., Ubele, M. F., Campbell, K. S., McCarthy,**
598 **J. J., Peterson, C. A. and Dupont-Versteegden, E. E.** (2012). Satellite cell depletion does
599 not inhibit adult skeletal muscle regrowth following unloading-induced atrophy. *Am J*
600 *Physiol Cell Physiol* **303**, C854-861.
- 601 **Joe, A. W., Yi, L., Natarajan, A., Le Grand, F., So, L., Wang, J., Rudnicki, M. A. and Rossi, F. M.**
602 (2010). Muscle injury activates resident fibro/adipogenic progenitors that facilitate
603 myogenesis. *Nat Cell Biol* **12**, 153-163.
- 604 **Keefe, A. C., Lawson, J. A., Flygare, S. D., Fox, Z. D., Colasanto, M. P., Mathew, S. J., Yandell,**
605 **M. and Kardon, G.** (2015). Muscle stem cells contribute to myofibres in sedentary adult
606 mice. *Nat Commun* **6**, 7087.
- 607 **Kuswanto, W., Burzyn, D., Panduro, M., Wang, K. K., Jang, Y. C., Wagers, A. J., Benoist, C. and**
608 **Mathis, D.** (2016). Poor Repair of Skeletal Muscle in Aging Mice Reflects a Defect in
609 Local, Interleukin-33-Dependent Accumulation of Regulatory T Cells. *Immunity* **44**, 355-
610 367.
- 611 **Lance-Jones, C.** (1988). The effect of somite manipulation on the development of motoneuron
612 projection patterns in the embryonic chick hindlimb. *Dev Biol* **126**, 408-419.
- 613 **Lepper, C. and Fan, C. M.** (2010). Inducible lineage tracing of Pax7-descendant cells reveals
614 embryonic origin of adult satellite cells. *Genesis* **48**, 424-436.
- 615 **Lepper, C., Partridge, T. A. and Fan, C. M.** (2011). An absolute requirement for Pax7-positive
616 satellite cells in acute injury-induced skeletal muscle regeneration. *Development* **138**,
617 3639-3646.
- 618 **Li, S., Karri, D., Sanchez-Ortiz, E., Jaichander, P., Bassel-Duby, R., Liu, N. and Olson, E. N.**
619 (2019). Sema3a-Nrp1 Signaling Mediates Fast-Twitch Myofiber Specificity of Tw2(+)
620 Cells. *Dev Cell* **51**, 89-98.e84.
- 621 **Liu, L., Cheung, T. H., Charville, G. W., Hurgo, B. M., Leavitt, T., Shih, J., Brunet, A. and Rando,**
622 **T. A.** (2013). Chromatin modifications as determinants of muscle stem cell quiescence
623 and chronological aging. *Cell Rep* **4**, 189-204.
- 624 **Liu, L., Cheung, T. H., Charville, G. W. and Rando, T. A.** (2015). Isolation of skeletal muscle stem
625 cells by fluorescence-activated cell sorting. *Nat Protoc* **10**, 1612-1624.
- 626 **Liu, N., Garry, G. A., Li, S., Bezprozvannaya, S., Sanchez-Ortiz, E., Chen, B., Shelton, J. M.,**
627 **Jaichander, P., Bassel-Duby, R. and Olson, E. N.** (2017). A Twist2-dependent progenitor
628 cell contributes to adult skeletal muscle. *Nat Cell Biol* **19**, 202-213.
- 629 **Madisen, L., Zwingman, T. A., Sunkin, S. M., Oh, S. W., Zariwala, H. A., Gu, H., Ng, L. L.,**
630 **Palmiter, R. D., Hawrylycz, M. J., Jones, A. R., et al.** (2010). A robust and high-
631 throughput Cre reporting and characterization system for the whole mouse brain.
632 *Nature Neuroscience* **13**, 133-140.
- 633 **Malecova, B. and Puri, P. L.** (2012). "Mix of Mics"- Phenotypic and Biological Heterogeneity of
634 "Multipotent" Muscle Interstitial Cells (MICs). *J Stem Cell Res Ther.*

- 635 **Mathew, S. J., Hansen, J. M., Merrell, A. J., Murphy, M. M., Lawson, J. A., Hutcheson, D. A.,**
636 **Hansen, M. S., Angus-Hill, M. and Kardon, G.** (2011). Connective tissue fibroblasts and
637 Tcf4 regulate myogenesis. *Development* **138**, 371-384.
- 638 **McCarthy, J. J., Mula, J., Miyazaki, M., Erfani, R., Garrison, K., Farooqui, A. B., Srikuea, R.,**
639 **Lawson, B. A., Grimes, B., Keller, C., et al.** (2011). Effective fiber hypertrophy in satellite
640 cell-depleted skeletal muscle. *Development* **138**, 3657-3666.
- 641 **Michaud, J. L., Lapointe, F. and Le Douarin, N. M.** (1997). The dorsoventral polarity of the
642 presumptive limb is determined by signals produced by the somites and by the lateral
643 somatopleure. *Development* **124**, 1453-1463.
- 644 **Mierzejewski, B., Archacka, K., Grabowska, I., Florkowska, A., Ciemerych, M. A. and Brzoska,**
645 **E.** (2020a). Human and mouse skeletal muscle stem and progenitor cells in health and
646 disease. *Semin Cell Dev Biol* **104**, 93-104.
- 647 **Mierzejewski, B., Grabowska, I., Jackowski, D., Irhashava, A., Michalska, Z., Stremińska, W.,**
648 **Jańczyk-Ilach, K., Ciemerych, M. A. and Brzoska, E.** (2020b). Mouse CD146+ muscle
649 interstitial progenitor cells differ from satellite cells and present myogenic potential.
650 *Stem Cell Res Ther* **11**, 341.
- 651 **Mitchell, K. J., Pannérec, A., Cadot, B., Parlakian, A., Besson, V., Gomes, E. R., Marazzi, G. and**
652 **Sassoon, D. A.** (2010). Identification and characterization of a non-satellite cell muscle
653 resident progenitor during postnatal development. *Nat Cell Biol* **12**, 257-266.
- 654 **Murach, K. A., Vechetti, I. J., Van Pelt, D. W., Crow, S. E., Dungan, C. M., Figueiredo, V. C.,**
655 **Kosmac, K., Fu, X., Richards, C. I., Fry, C. S., et al.** (2020). Fusion-Independent Satellite
656 Cell Communication to Muscle Fibers During Load-Induced Hypertrophy. *Function (Oxf)*
657 **1**, zqaa009.
- 658 **Murphy, M. M., Lawson, J. A., Mathew, S. J., Hutcheson, D. A. and Kardon, G.** (2011). Satellite
659 cells, connective tissue fibroblasts and their interactions are crucial for muscle
660 regeneration. *Development* **138**, 3625-3637.
- 661 **Nassari, S., Duprez, D. and Fournier-Thibault, C.** (2017). Non-myogenic Contribution to Muscle
662 Development and Homeostasis: The Role of Connective Tissues. *Front Cell Dev Biol* **5**, 22.
- 663 **Nelson, L. T., Rakshit, S., Sun, H. and Wellik, D. M.** (2008). Generation and expression of a
664 Hoxa11eGFP targeted allele in mice. *Dev Dyn* **237**, 3410-3416.
- 665 **Pawlikowski, B., Pulliam, C., Betta, N. D., Kardon, G. and Olwin, B. B.** (2015). Pervasive satellite
666 cell contribution to uninjured adult muscle fibers. *Skelet Muscle* **5**, 42.
- 667 **Pineault, K. M., Song, J. Y., Kozloff, K. M., Lucas, D. and Wellik, D. M.** (2019). Hox11 expressing
668 regional skeletal stem cells are progenitors for osteoblasts, chondrocytes and
669 adipocytes throughout life. *Nat Commun* **10**, 3168.
- 670 **Qu-Petersen, Z., Deasy, B., Jankowski, R., Ikezawa, M., Cummins, J., Pruchnic, R., Mytinger, J.,**
671 **Cao, B., Gates, C., Wernig, A., et al.** (2002). Identification of a novel population of
672 muscle stem cells in mice: potential for muscle regeneration. *J Cell Biol* **157**, 851-864.
- 673 **Rivers, L. E., Young, K. M., Rizzi, M., Jamen, F., Psachoulia, K., Wade, A., Kessar, N. and**
674 **Richardson, W. D.** (2008). PDGFRA/NG2 glia generate myelinating oligodendrocytes and
675 piriform projection neurons in adult mice. *Nat Neurosci* **11**, 1392-1401.
- 676 **Sambasivan, R., Yao, R., Kissenpfennig, A., Van Wittenberghe, L., Paldi, A., Gayraud-Morel, B.,**
677 **Guenou, H., Malissen, B., Tajbakhsh, S. and Galy, A.** (2011). Pax7-expressing satellite

- 678 cells are indispensable for adult skeletal muscle regeneration. *Development* **138**, 3647-
679 3656.
- 680 **Sefton, E. M. and Kardon, G.** (2019). Connecting muscle development, birth defects, and
681 evolution: An essential role for muscle connective tissue. *Curr Top Dev Biol* **132**, 137-
682 176.
- 683 **Swinehart, I. T., Schlientz, A. J., Quintanilla, C. A., Mortlock, D. P. and Wellik, D. M.** (2013).
684 Hox11 genes are required for regional patterning and integration of muscle, tendon and
685 bone. *Development* **140**, 4574-4582.
- 686 **Tatsumi, R., Sankoda, Y., Anderson, J. E., Sato, Y., Mizunoya, W., Shimizu, N., Suzuki, T.,**
687 **Yamada, M., Rhoads, R. P., Ikeuchi, Y., et al.** (2009). Possible implication of satellite
688 cells in regenerative motoneuritogenesis: HGF upregulates neural chemorepellent
689 *Sema3A* during myogenic differentiation. *Am J Physiol Cell Physiol* **297**, C238-252.
- 690 **Tedesco, F. S., Moyle, L. A. and Perdiguero, E.** (2017). Muscle Interstitial Cells: A Brief Field
691 Guide to Non-satellite Cell Populations in Skeletal Muscle. *Methods Mol Biol* **1556**, 129-
692 147.
- 693 **Thomas, K., Engler, A. J. and Meyer, G. A.** (2015). Extracellular matrix regulation in the muscle
694 satellite cell niche. *Connect Tissue Res* **56**, 1-8.
- 695 **Tidball, J. G. and Villalta, S. A.** (2010). Regulatory interactions between muscle and the immune
696 system during muscle regeneration. *Am J Physiol Regul Integr Comp Physiol* **298**, R1173-
697 1187.
- 698 **Uezumi, A., Fukada, S., Yamamoto, N., Takeda, S. and Tsuchida, K.** (2010). Mesenchymal
699 progenitors distinct from satellite cells contribute to ectopic fat cell formation in skeletal
700 muscle. *Nat Cell Biol* **12**, 143-152.
- 701 **Uezumi, A., Ito, T., Morikawa, D., Shimizu, N., Yoneda, T., Segawa, M., Yamaguchi, M.,**
702 **Ogawa, R., Matev, M. M., Miyagoe-Suzuki, Y., et al.** (2011). Fibrosis and adipogenesis
703 originate from a common mesenchymal progenitor in skeletal muscle. *J Cell Sci* **124**,
704 3654-3664.
- 705 **Wellik, D. M. and Capecchi, M. R.** (2003). Hox10 and Hox11 genes are required to globally
706 pattern the mammalian skeleton. *Science* **301**, 363-367.
- 707 **Yin, H., Price, F. and Rudnicki, M. A.** (2013). Satellite cells and the muscle stem cell niche.
708 *Physiol Rev* **93**, 23-67.
709

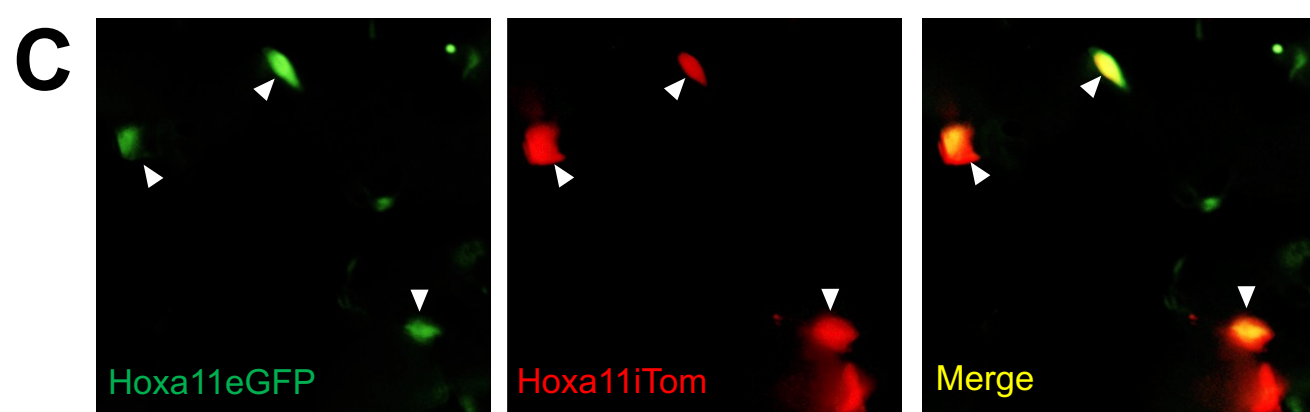
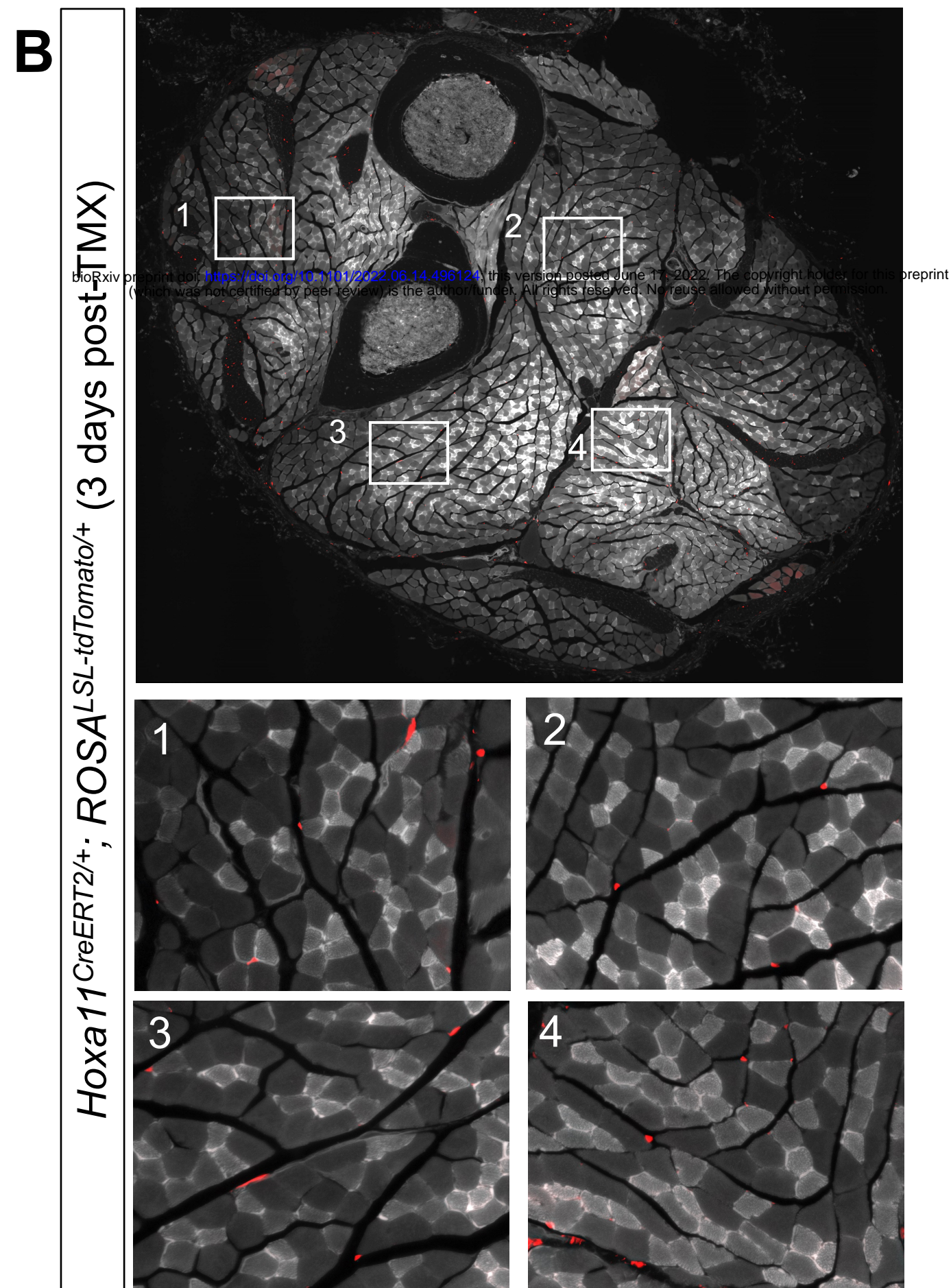
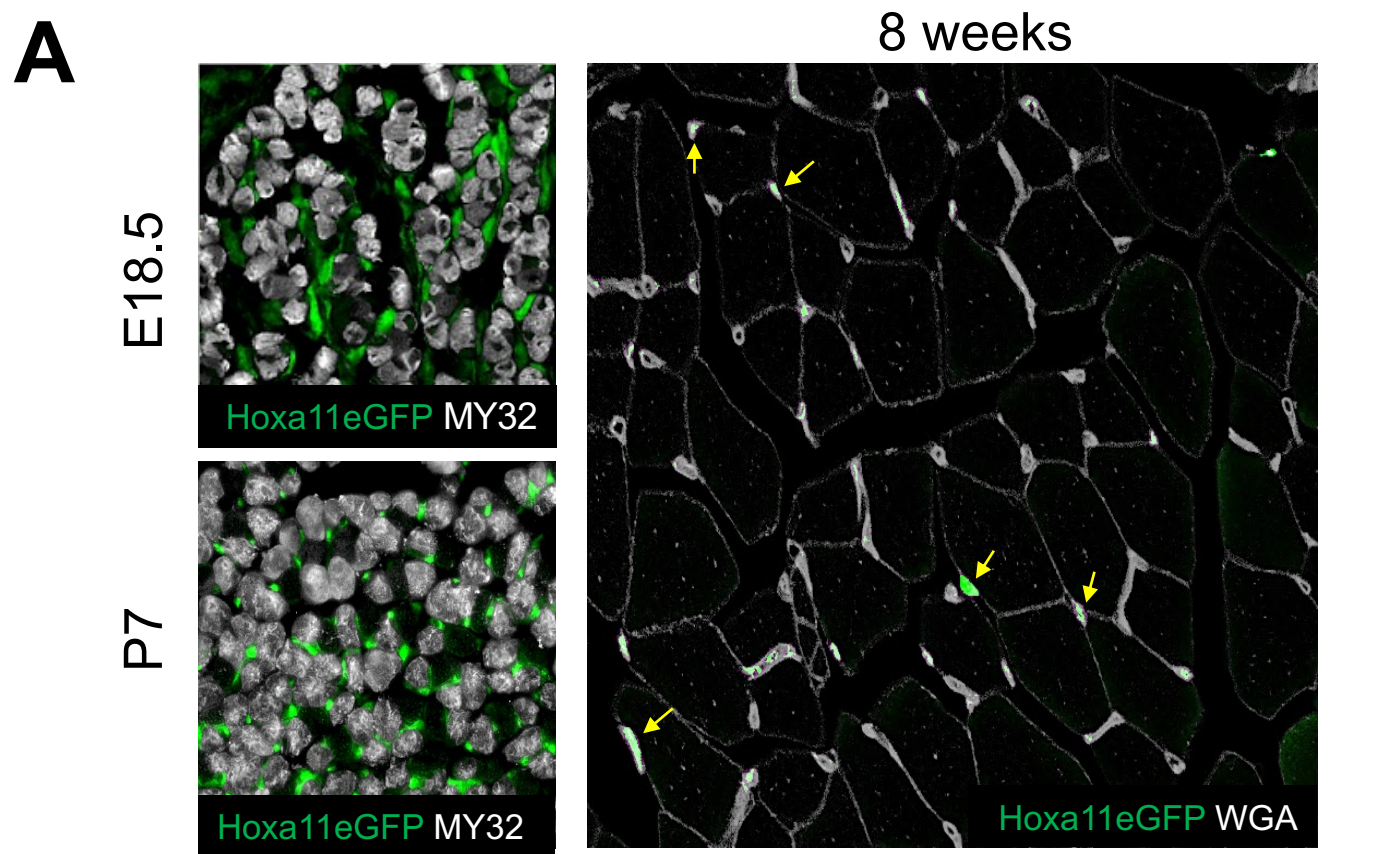
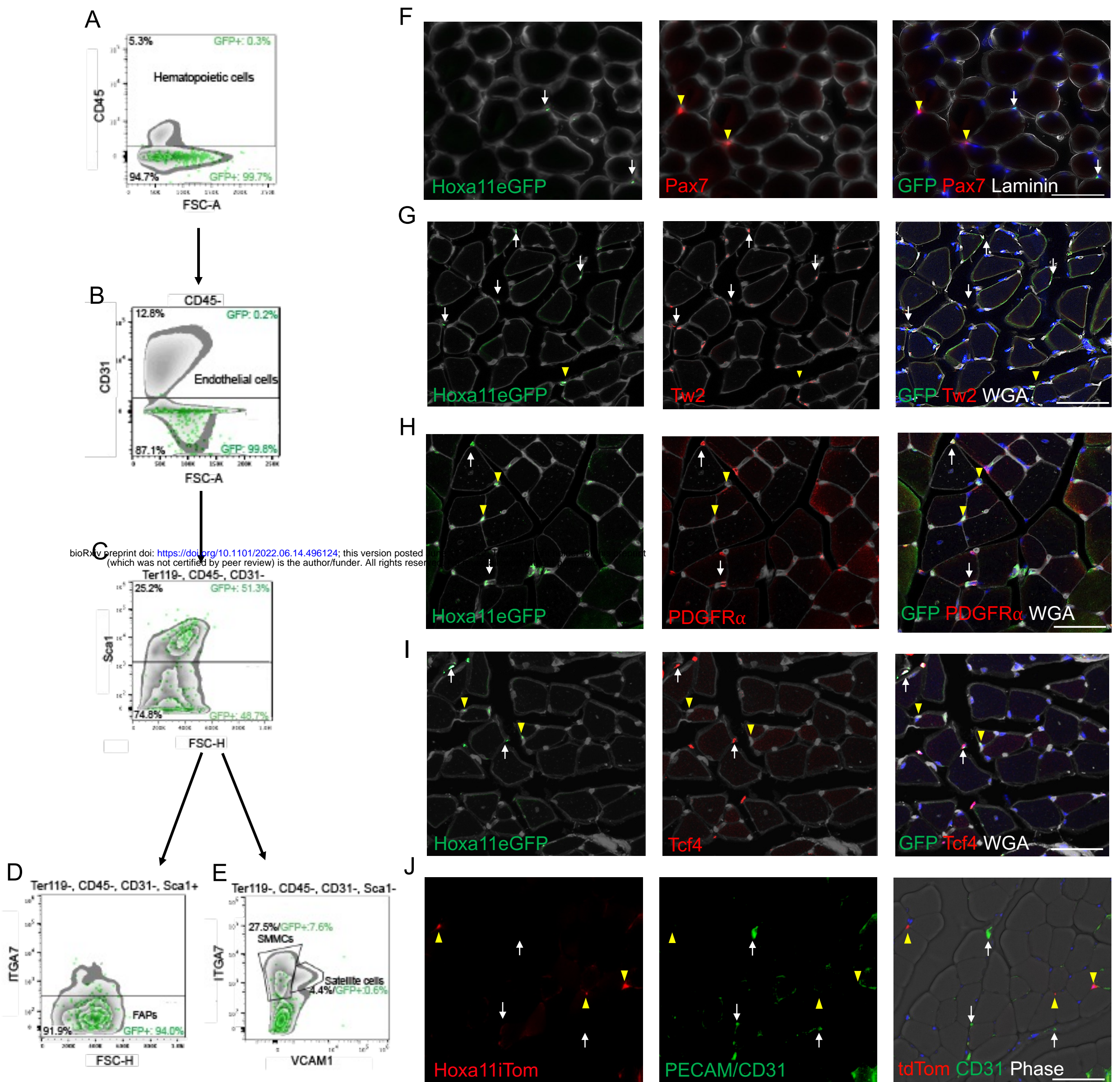


Figure 1. Hoxa11 expression is maintained in skeletal muscle interstitial cells throughout life. (A) Hoxa11eGFP real-time reporter shows expression (green) at E18.5 and P7 surrounding muscle fibers (MY32, white). At 8 weeks of age, Hoxa11eGFP (green, yellow arrows) is expressed in the interstitium visualized with WGA (white). **(B)** High magnification images from a whole forelimb cross section show tdTomato expression (Hoxa11iTom, red) in the interstitium throughout forelimb muscles. **(C)** Hoxa11 lineage reporter (Hoxa11iTom, red) overlaps with real-time reporter Hoxa11eGFP (green, white arrowheads) in interstitial cells 3 days post-tamoxifen.



bioRxiv preprint doi: <https://doi.org/10.1101/2022.06.14.496124>; this version posted (which was not certified by peer review) is the author/funder. All rights reserved.

Figure 2. Hoxa11eGFP-positive cells are a subset of interstitial cells. Flow cytometric analyses of mononucleated live cells from zeugopod muscles of 14-week-old mice stained with CD45, TER119, CD31, Sca1, Itga7 and VCAM1. After sorting by forward scatter, side scatter and using DAPI for exclusion of dead cells, Hoxa11eGFP⁺ cells sort as non-hematopoietic (CD45⁻ and TER119-negative), (A), and non-endothelial (CD31-negative), (B). (C) Within the non-hematopoietic, non-endothelial population, Hoxa11eGFP⁺ cells sort as 51% Sca1-positive and 49% Sca1-negative cells. (D) The majority of Hoxa11eGFP⁺/Sca1⁺ cells are Itga7-negative (FAPs). (E) The Hoxa11eGFP⁺/Sca1⁻ population is negative for VCAM1, and Hoxa11eGFP⁺/Sca1⁻ cells do not sort with the Itga7⁺/VCAM⁺ satellite cells. Approximately 8% of the Hoxa11eGFP⁺/Sca1⁻ cells are Itga7⁺/VCAM⁻, a marker combination used to identify SMMCs. Hoxa11eGFP⁺ cells are represented as green dots on top of gray-scale density plots of non-GFP labeled cells. Forelimb ventral muscle sections of 8–10-week-old animals were immunostained for GFP, Pax7 and WGA (F); GFP, Twist2 and WGA (G); GFP, PDGFR α and WGA (H); GFP, Tcf4 and WGA (I). (F) Hox11eGFP⁺ (arrows) cells do not overlap with Pax7⁺ satellite cells (arrowheads). Arrows (white) in G–J indicate double positive cells. Arrowheads (yellow) in G–J indicate Hox11eGFP⁺ cells. (J) Hoxa11 lineage positive cells (Hoxa11iTom, arrows), 4-days post tamoxifen, do not colocalize with PECAM/CD31 (arrowheads). Scale bars, 50 μ m.

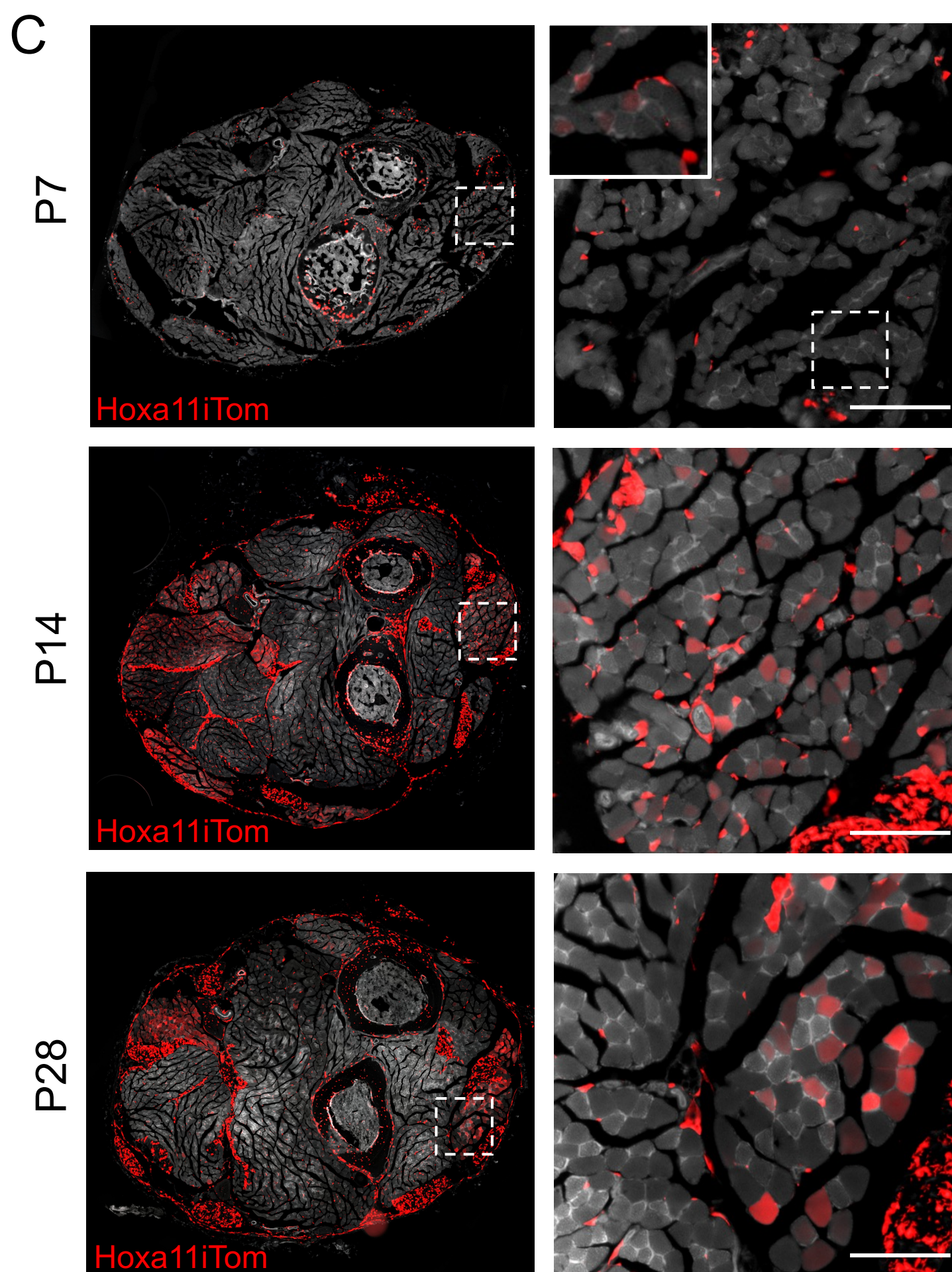
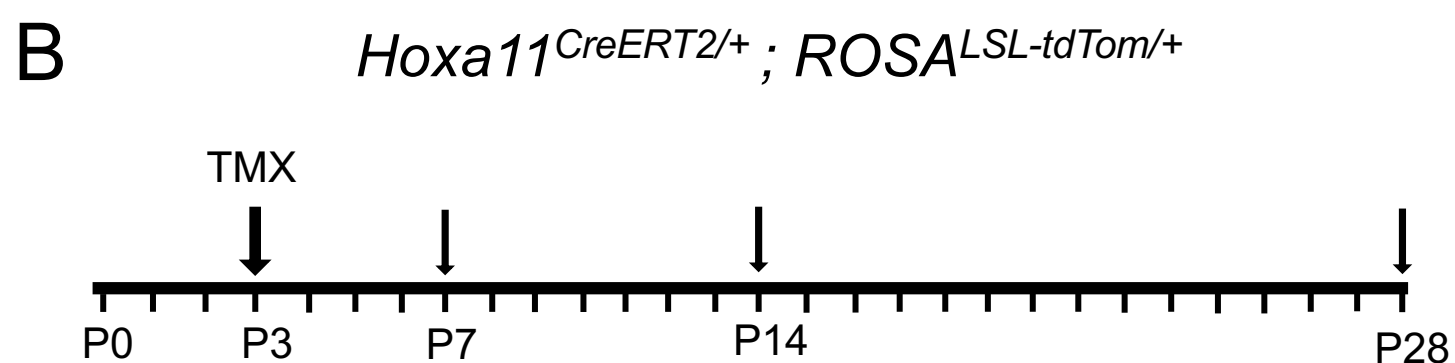
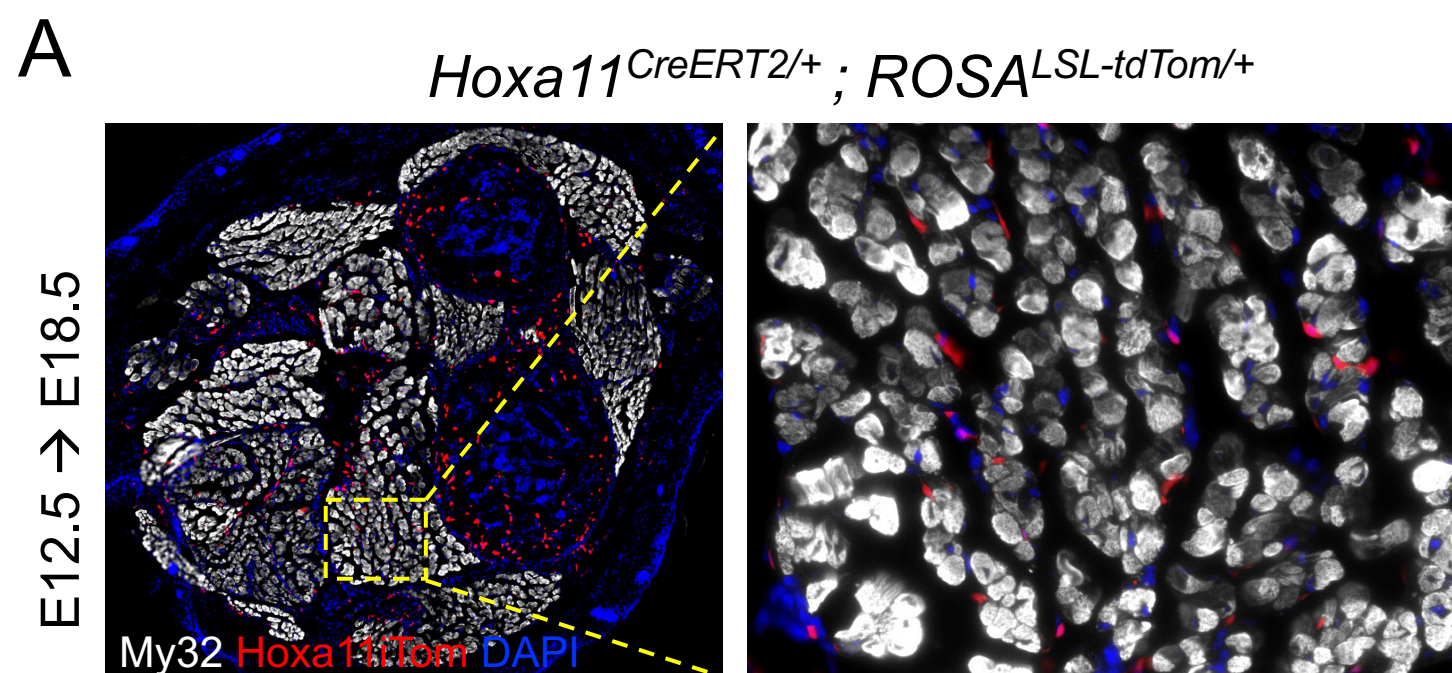


Figure 3. Embryonic *Hoxa11* lineage is exclusively interstitial; postnatal lineage begins to contribute to myofibers. At E12.5 the pregnant dams were dosed with 5mg Tamoxifen by intraperitoneal injection and embryos were collected at E18.5. **(A)** Representative cross-section of E18.5 forelimb stained for My32 (white) with Hoxa11iTom (red) visible in connective tissue and bone; nuclear staining shown with DAPI (blue). High magnification of E18.5 forelimb muscle shows tdTomato signal does not overlap with My32. **(B)** At postnatal day 3 *Hoxa11^{CreERT2/+}; ROSA^{LSL-tdTom/+}* mice were given 0.25mg Tamoxifen by intragastric injection and collected at P7, P14, and P28. **(C)** Full forelimb cross sections show tdTom (Hoxa11iTom) expression throughout forelimb tissues and high magnification images show clear tdTom expression in myofibers at P14 and P28. Inset of P7 muscle shows some faint tdTom⁺ myofibers when imaged at a higher exposure. Scale bars, 100µm.

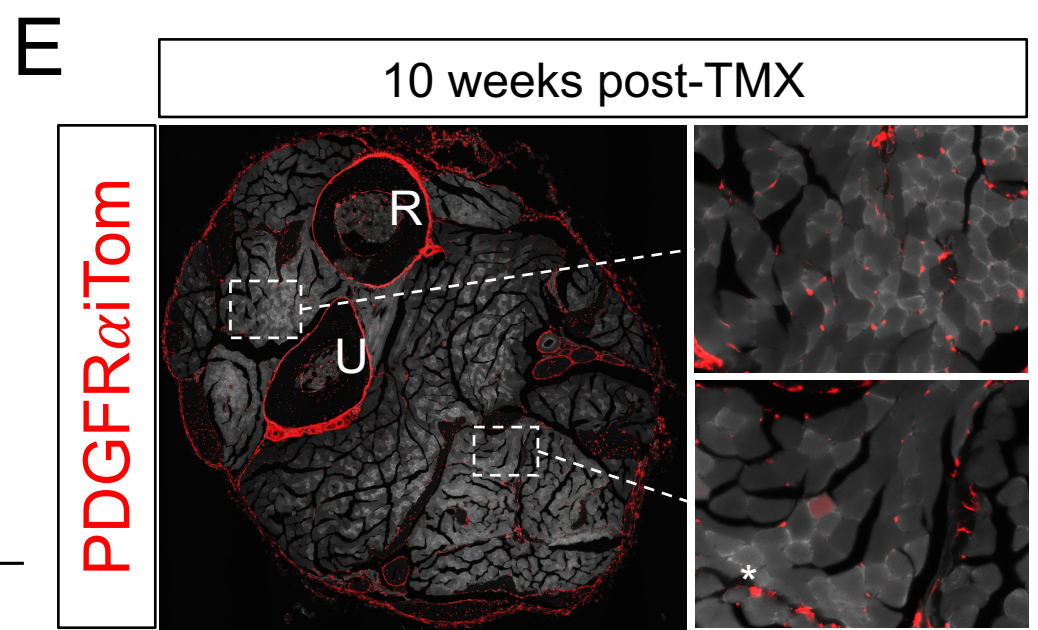
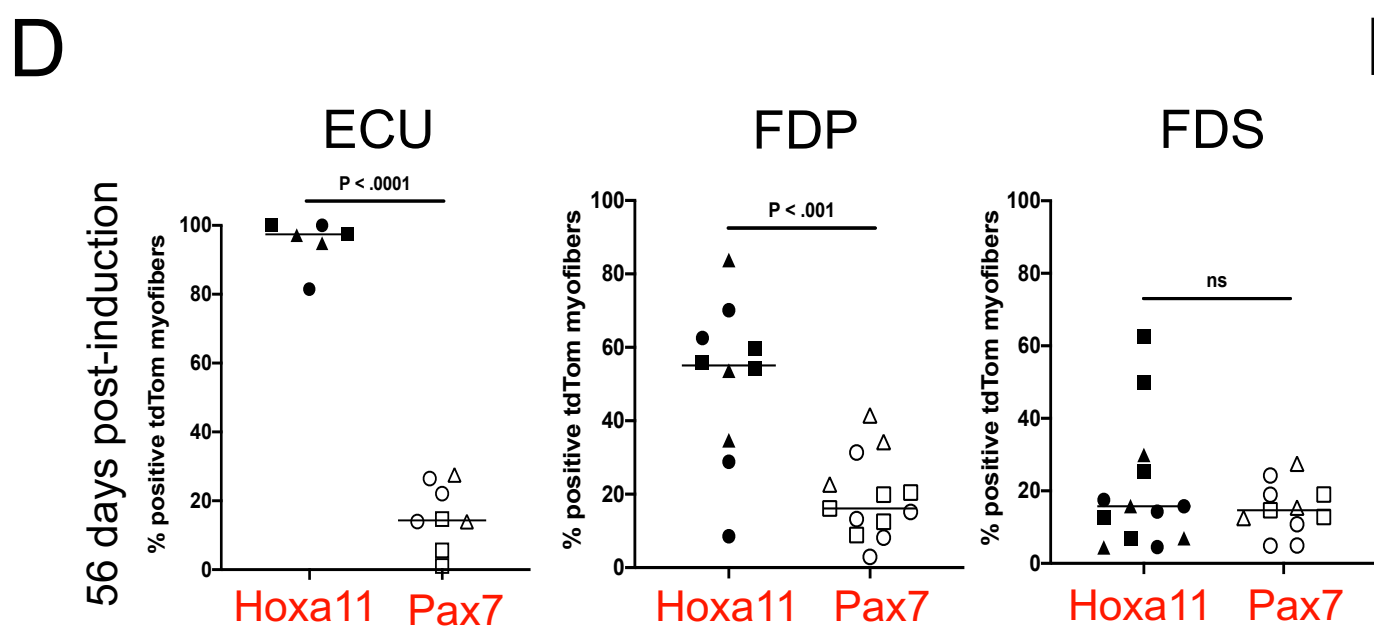
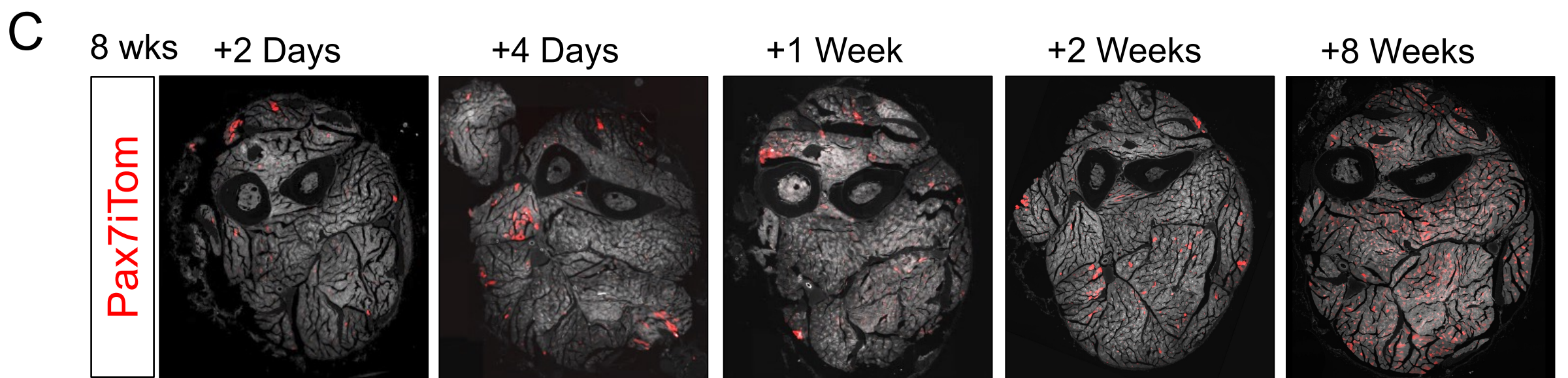
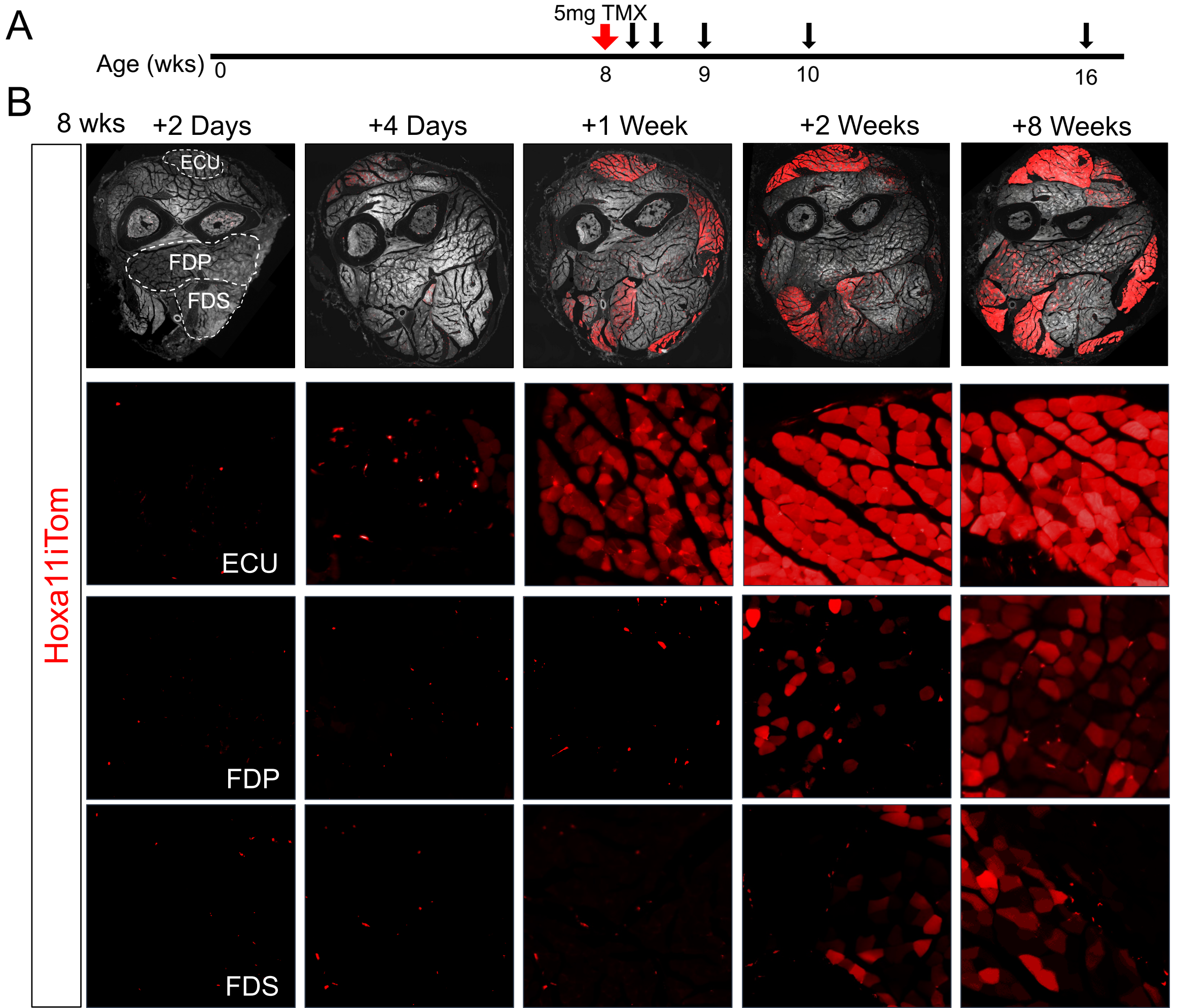
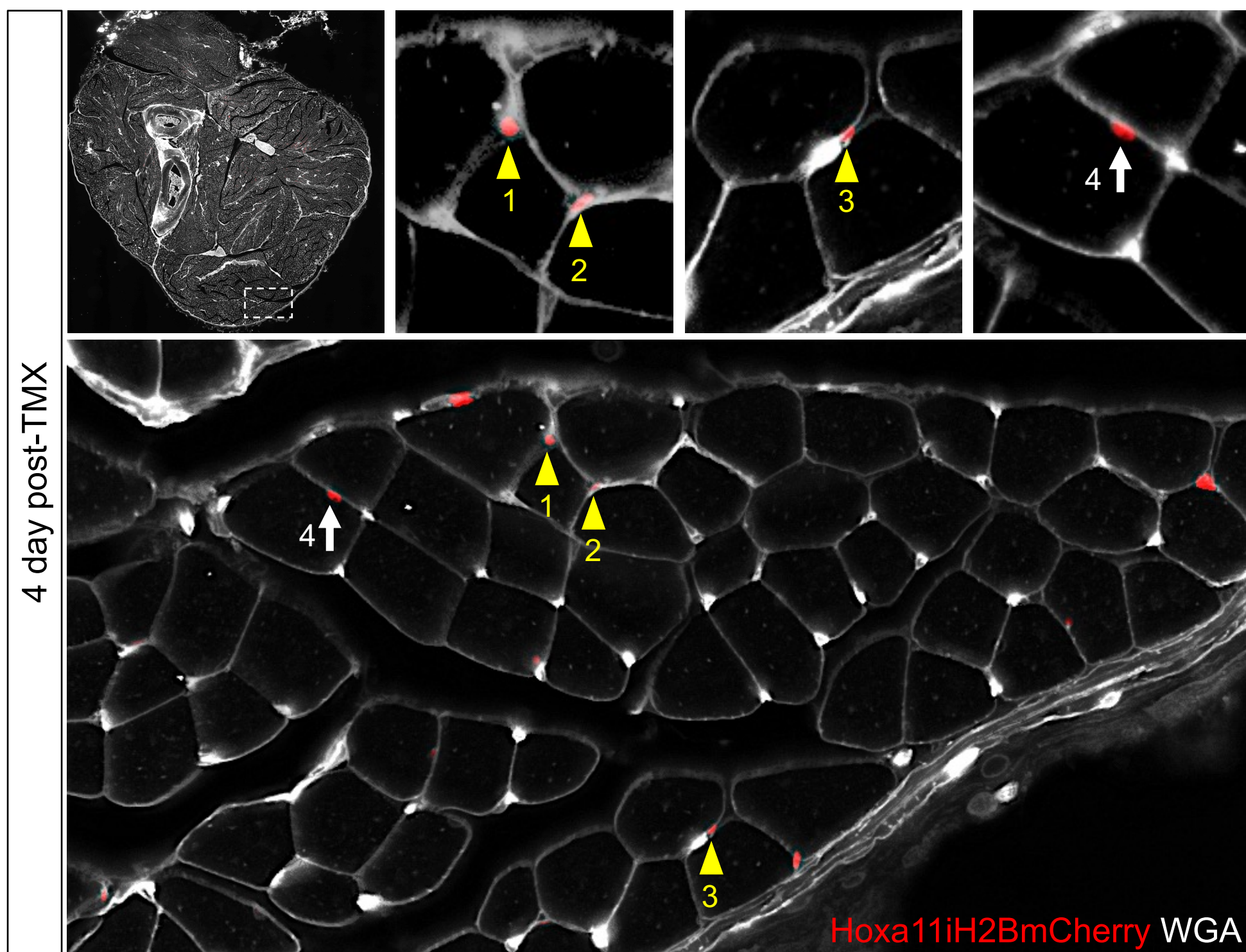


Figure 4. Hoxa11-expressing skeletal muscle interstitial cells progressively contribute to myofibers in the adult mouse forelimb. (A) *Hoxa11^{CreERT2/eGFP}; ROSA^{LSL-TdTom}/+* (Hoxa11iTom) mice were given a single intraperitoneal injection of 5 mg tamoxifen at 8 weeks of age and collected at 2 days, 4 days, 1 week, 2 weeks, and 8 weeks after tamoxifen induction. (B) Whole forelimb cross-sections were collected at time points indicated. Images of Extensor Carpi Ulnaris (ECU), Flexor Digitorum Profundus (FDP), and Flexor Digitorum Sublimis (FDS) muscles from Hoxa11iTom muscle show increasing number of tdTomato expressing myofibers over time. (C) Full forelimb cross-sections from *Pax7^{CreERT2/+}; ROSA^{LSL-TdTom}/+* (Pax7iTom) animals shows fewer tdTomato positive myofibers compared to Hoxa11iTom animals at the same time points. (D) Quantification of percentage tdTomato-positive myofibers from ECU, FDS, and FDP muscles from Hoxa11iTom and Pax7iTom animals 8 weeks post-induction (n=3 animals, 2-5 fields of view per muscle group analyzed). Statistics by Student's t-test. ns, not significant. White dashed line marks borders of muscles shown in B and quantified in D, position of radius and ulna marked by R and U, respectively. (E) *PDGFR α ^{CreERT2/+}; ROSA^{LSL-tdTomato/+}* (PDGFR α iTom) animals were treated with 5 mg tamoxifen at 8 weeks of age and collected 10 weeks later. Whole cross section of the forelimb shows tdTomato expression in connective tissues, bone tissue, tendons, and the muscle interstitium. High magnification images of skeletal muscle shows PDGFR α iTom expression in the muscle interstitium. A few myofibers were noticed to have low tdTomato expression marked by asterisks (*).

A

Hoxa11^{CreERT2/+}; *ROSA*^{LSL-H2BmCherry/+}

B



C

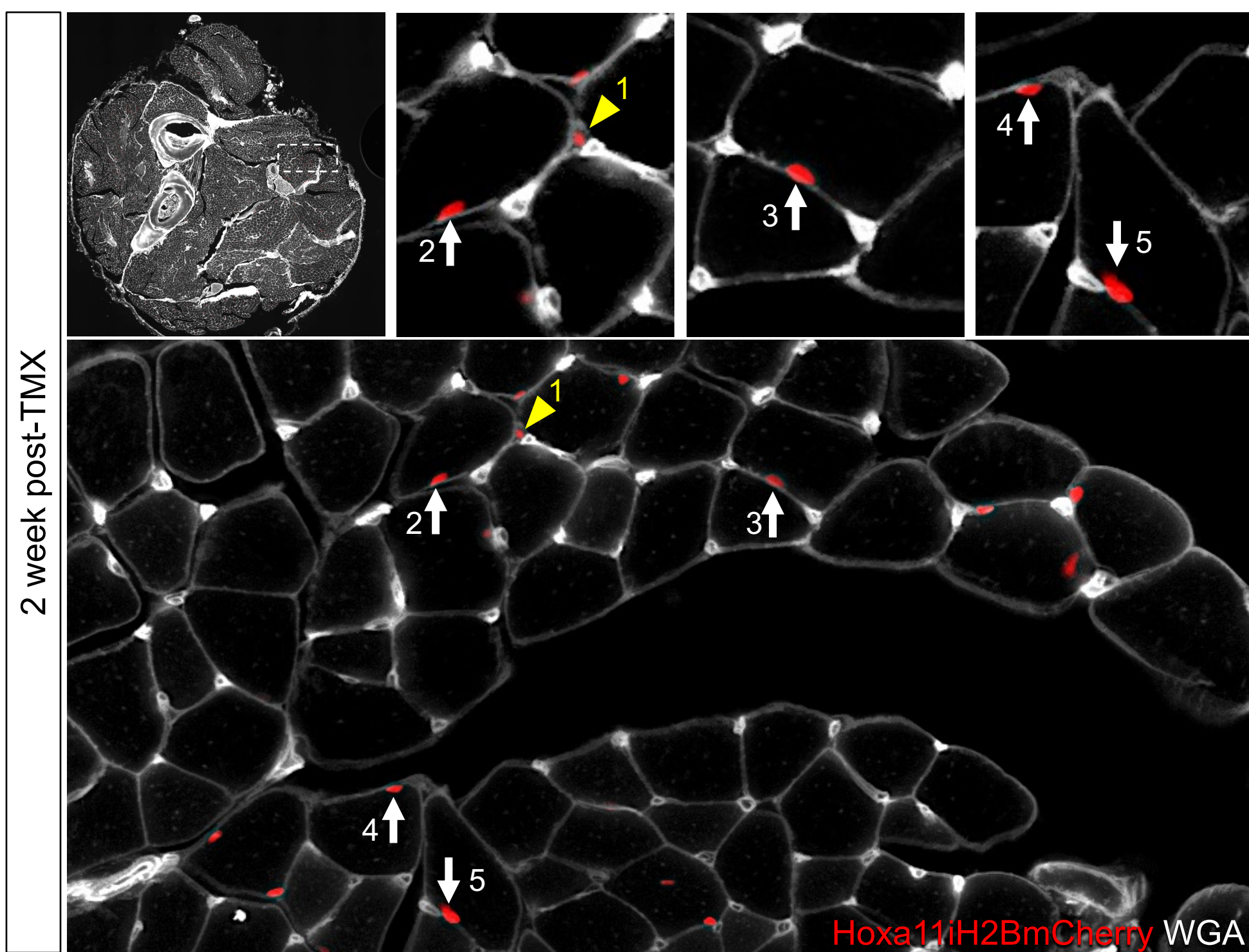


Figure 5. Hoxa11-expressing interstitial cells contribute their nuclei to myofibers. (A) *Hoxa11^{CreERT2/+}; ROSA^{LSL-H2BmCherry/+}* mice were given 5mg of tamoxifen at 6 weeks of age and collected 4 days and 2 weeks after dosing. (B) Top, left image shows a cross section of the forelimb of an adult mouse 4-days post-tamoxifen dosing. The larger, bottom image is a higher magnification image of the tissue in the white dashed box. The three top, right images are high resolution pictures of interstitial or myofiber nuclei from the bottom panel. (C) Top, left image shows a cross section of the forelimb of an adult mouse 2-weeks post-tamoxifen dosing. The larger, bottom image is a higher magnification image of the tissue in the white dashed box. The three top, right images are high resolution pictures of interstitial or myofiber nuclei from the bottom panel. Yellow arrowheads point to H2BmCherry labeled interstitial cell nuclei; white arrows point to H2BmCherry labeled myonuclei in **B** and **C**.

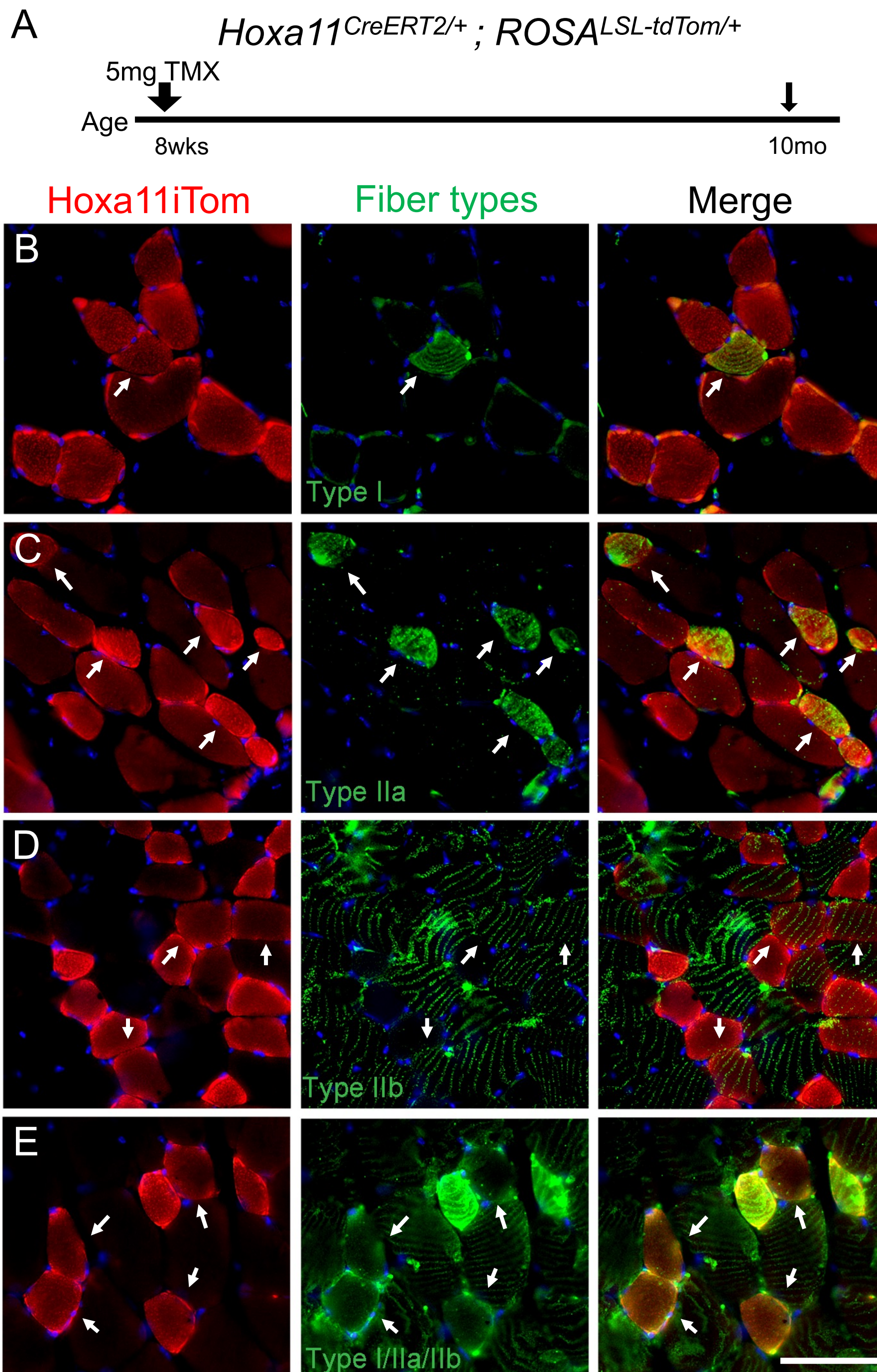
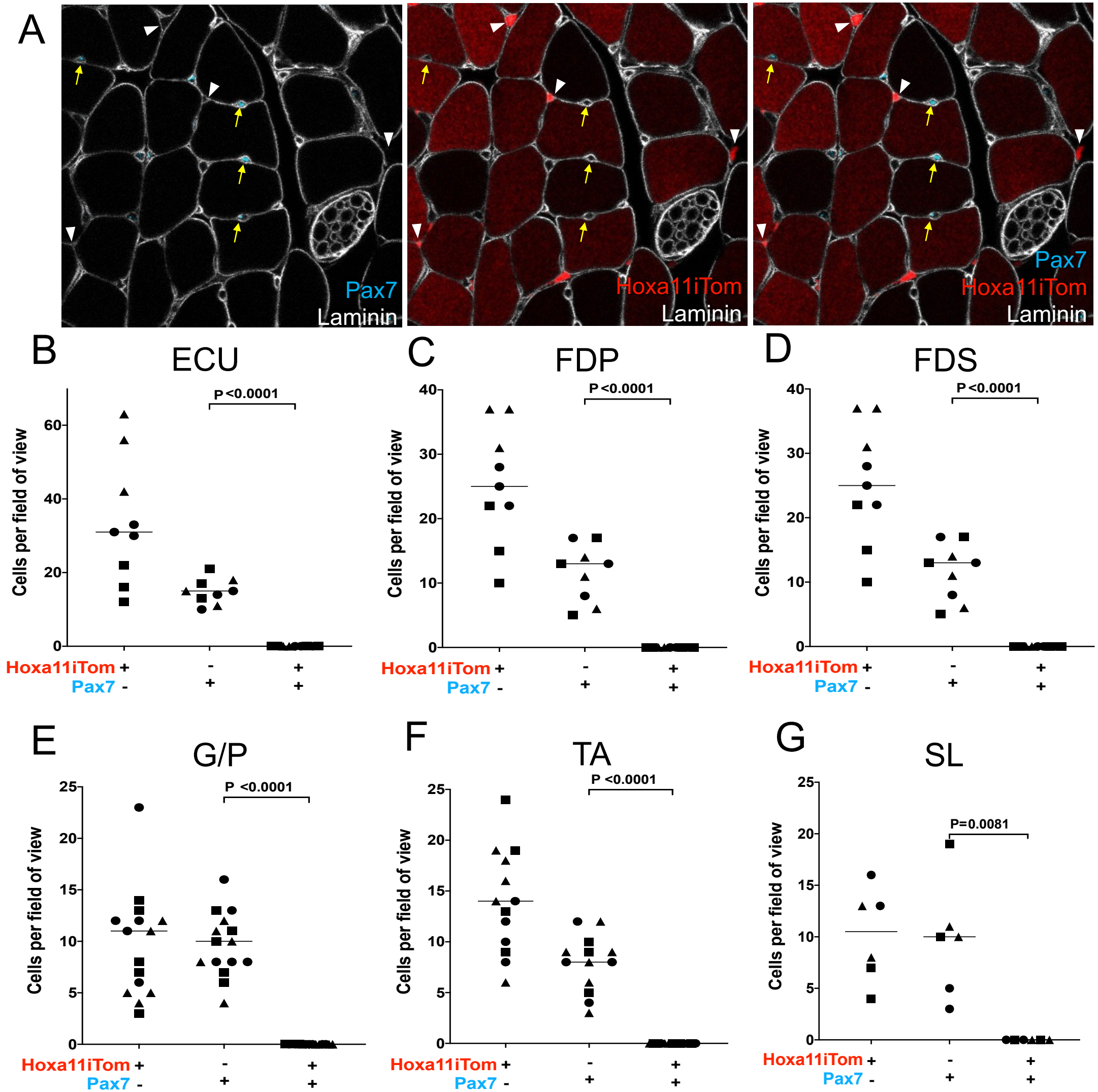


Figure 6. *Hoxa11* lineage contributes to Type I, Type IIa, Type IIb, and Type IIx myofibers. (A) Mice were treated with tamoxifen at 8-weeks of age and collected at 10 months of age. (B-D) *Hoxa11* lineage labeled myofibers are identified by tdTomato signal (*Hoxa11iTom*). Myofiber sub-types were identified by immunofluorescent staining with anti-myosin (Slow), anti-SC-71, and anti-BF-F3 (additional antibody details are available in Supplemental Table 1). (E) Type IIx fibers were identified by the absence of combined markers. Fibers shown are from the Gastrocnemius/Plantaris muscles. Lineage labeling is observed in all myofiber sub-types (white arrows). Scale bar = 100 μ m.

Hoxa11^{CreERT2/eGFP}; *ROSA*^{LSL-tdTom/+}
2 weeks post-Tmx



H

Hoxa11^{CreERT2/+}; *ROSA*^{LSL-H2B-mCherry/+}
2 weeks post-Tmx

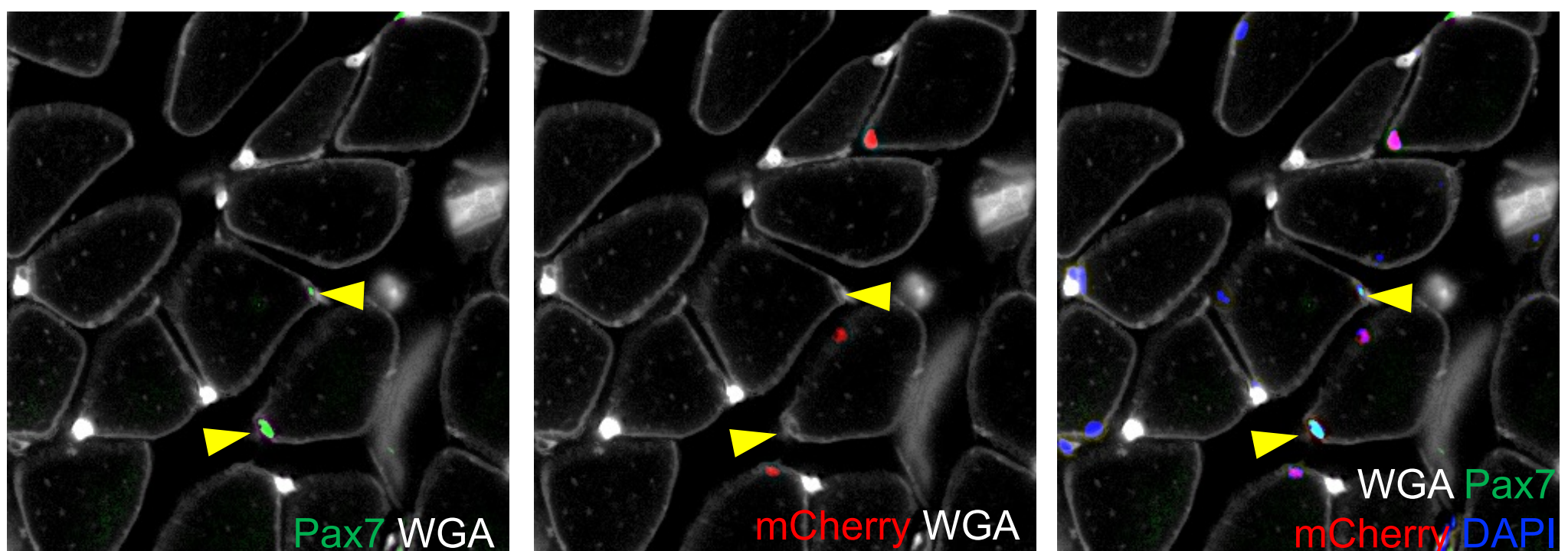


Figure 7. Pax7-expressing satellite cells are not lineage labeled by Hoxa11 lineage. *Hoxa11^{CreERT2/+}; ROSA^{LSL-tdTom/+}* mice given a single 5mg dose of tamoxifen by intraperitoneal injection at 8 or 12 weeks of age were collected 2-weeks later. **(A)** Pax7 cells (cyan, yellow arrows) are visualized under the basal lamina (white) with zero incidences of Hoxa11 lineage labeling (red) of Pax7-expressing cells in forelimb skeletal muscle at 2 weeks post-induction. **(B-G)**. The number of Hoxa11iTom and Pax7 single- or double-positive cells were quantified in the Extensor Carpi Ulnaris (ECU), Flexor Digitorum Profundus (FDP), and Flexor Digitorum Sublimis (FDS) muscles of the forelimb and the Gastrocnemius/Plantaris (G/P), Soleus (SL), and Tibialis Anterior (TA) muscles of the hindlimb. **(H)** *Hoxa11^{CreERT2/+}; ROSA^{LSL-H2B-mCherry/+}* animals were given a single 5mg dose of tamoxifen by intraperitoneal injection at 6 weeks of age and immunostained for Pax7+ satellite cells 2 weeks after dosing; no overlap of Hoxa11iH2BmCherry and Pax7 were observed.

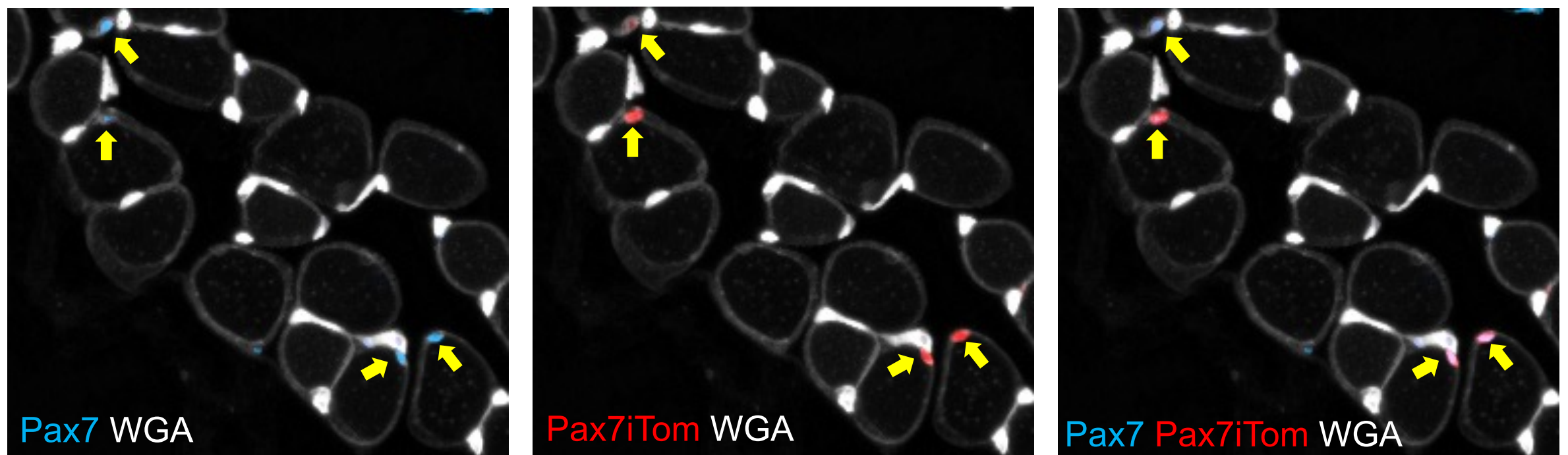
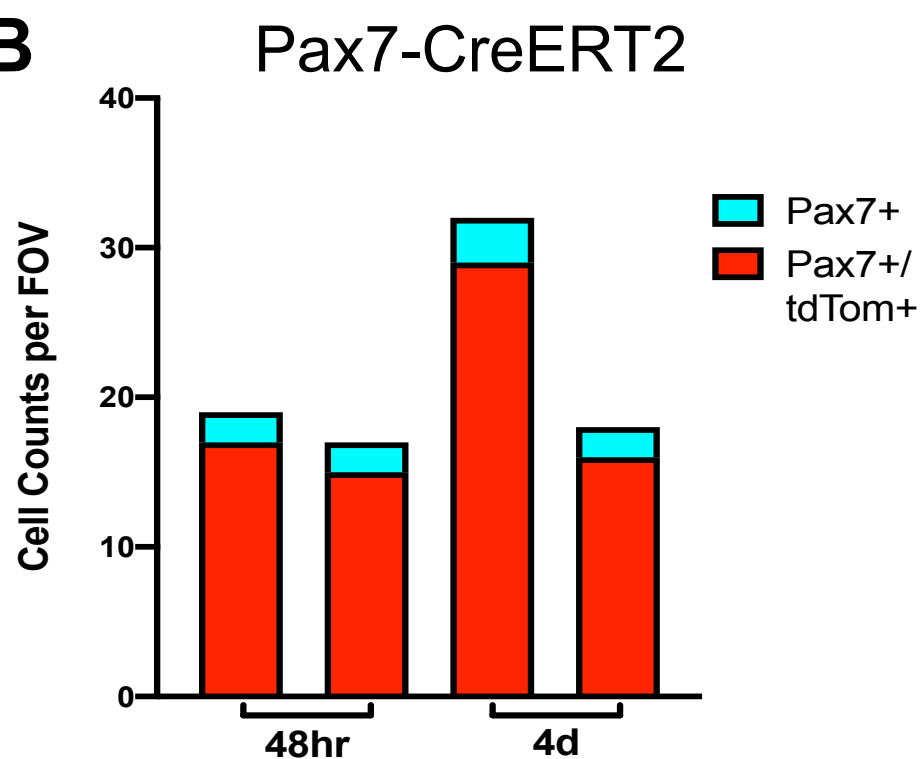
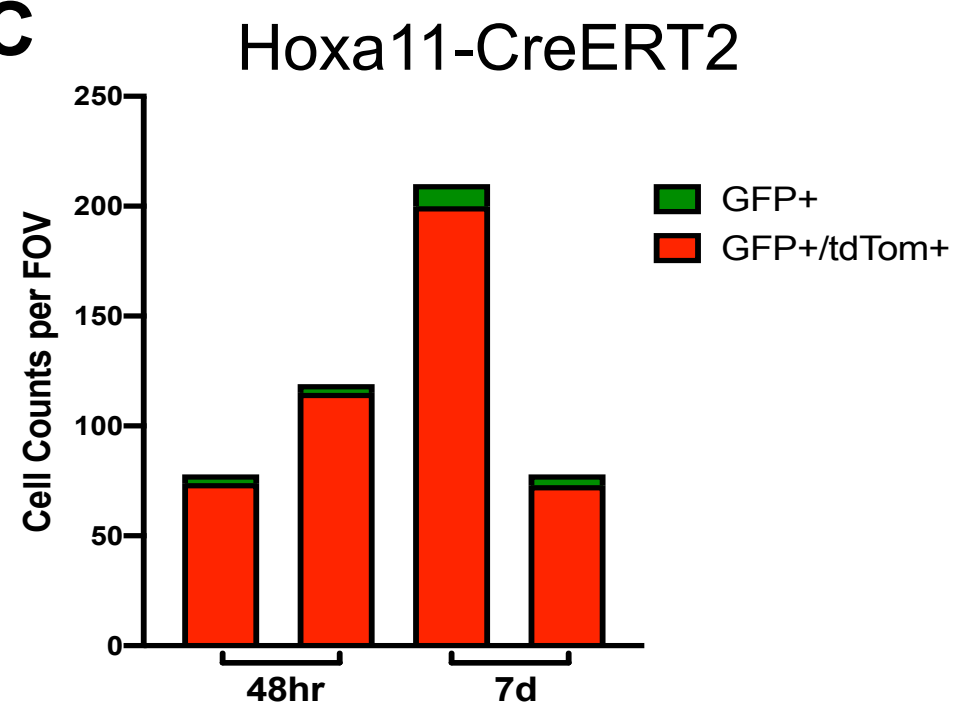
A**B****C**

Figure S1. Both *Hoxa11-CreERT2* and *Pax7-CreERT2* show approximately 90% efficiency with lineage reporter ROSA-LSL-tdTomato. (A) Images show Pax7 IF staining (blue) overlaps with tdTomato (red) in Pax7 lineage reporter animals (Pax7iTom) 4 days after tamoxifen treatment. (B) Quantification of Pax7-CreERT2 efficiency was assessed by counting the number of Pax7 antibody-stained cells and tdTomato labeled cells at 48hrs (n= 2 animals) and 4 days (n= 2 animals) after Tamoxifen treatment. (C) Quantification of Hoxa11-CreERT2-induced recombination of ROSA-LSL-tdTomato with a single 5mg bolus of tamoxifen was assessed by counting the number of Hoxa11eGFP and tdTomato labeled cells at 48hrs (n=2 animals) and 7 days (n=2 animals) after tamoxifen administration. Both Cres resulted in approximately 90% efficiency.

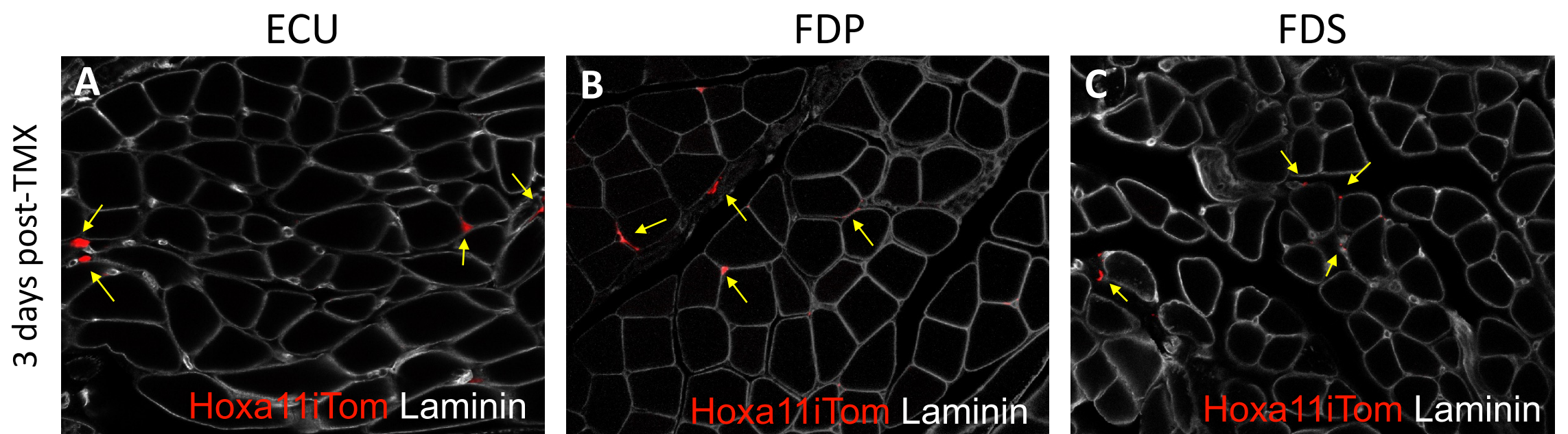


Figure S2. Hoxa11 expressing cells are only in the interstitium of zeugopod-attached muscles after initial recombination. Hoxa11 lineage labeling (Hoxa11iTom, red) is observed 3 days following tamoxifen administration. (A-C) Hoxa11 lineage-labeled cells are only seen in the interstitium (yellow arrows) of the Extensor Carpi Ulnaris (ECU), Flexor Digitorum Profundus (FDP) and Flexor Digitorum Sublimis (FDS) as shown by laminin (white).

Hoxa11-CreERT2; ROSA-LSL-tdTom

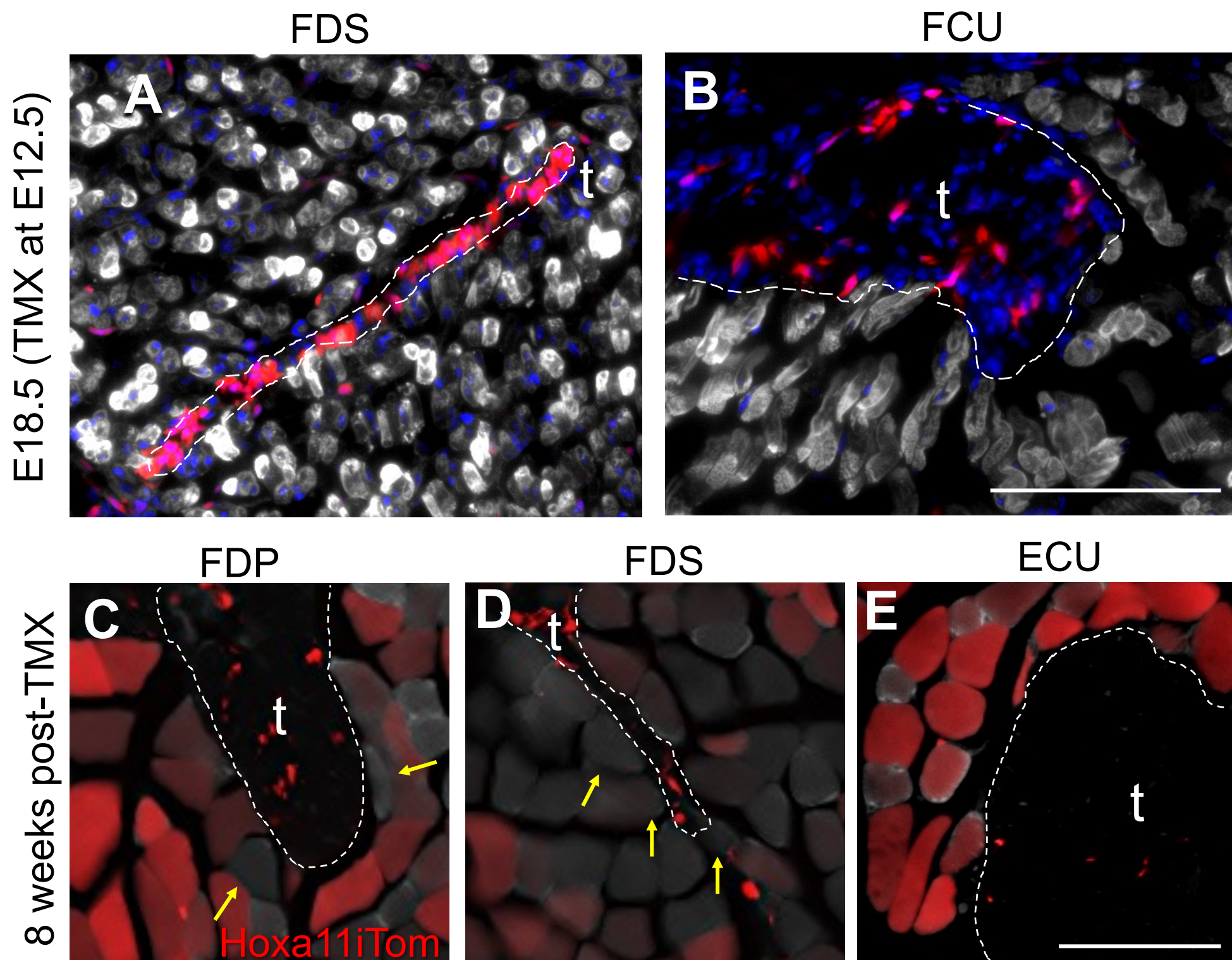


Figure S3. *Hoxa11* lineage shows no preferential contribution to myofibers near the myotendinous junctions during embryogenesis or homeostasis. Sections of embryonic forelimb muscles were analyzed for myofiber lineage contribution at E18.5. (A, B) Images of the Flexor Digitorum Sublimis (FDS) and Flexor Carpi Ulnaris (FCU) muscles at the myotendinous junction show no *Hoxa11*iTom (red) overlap with My32 (white), consistent with lineage labeling throughout the rest of the muscle body. Sections from adult *Hoxa11*iTom muscle of the Flexor Digitorum Profundus (FDP), Flexor Digitorum Sublimis (FDS), and Extensor Carpi Ulnaris were analyzed for *Hox11* lineage contribution at the myotendinous junction 8 weeks after the induction of lineage reporting. High magnification images show similar lineage labeling near the myotendinous junction FDP (C), FDS (D), or ECU (E) as in the mid-body of the muscle (Figure 4). Scale bars = 100µm. Tendons are marked with a t.

24 weeks post-TMX

Hoxa11iTom Background DAPI

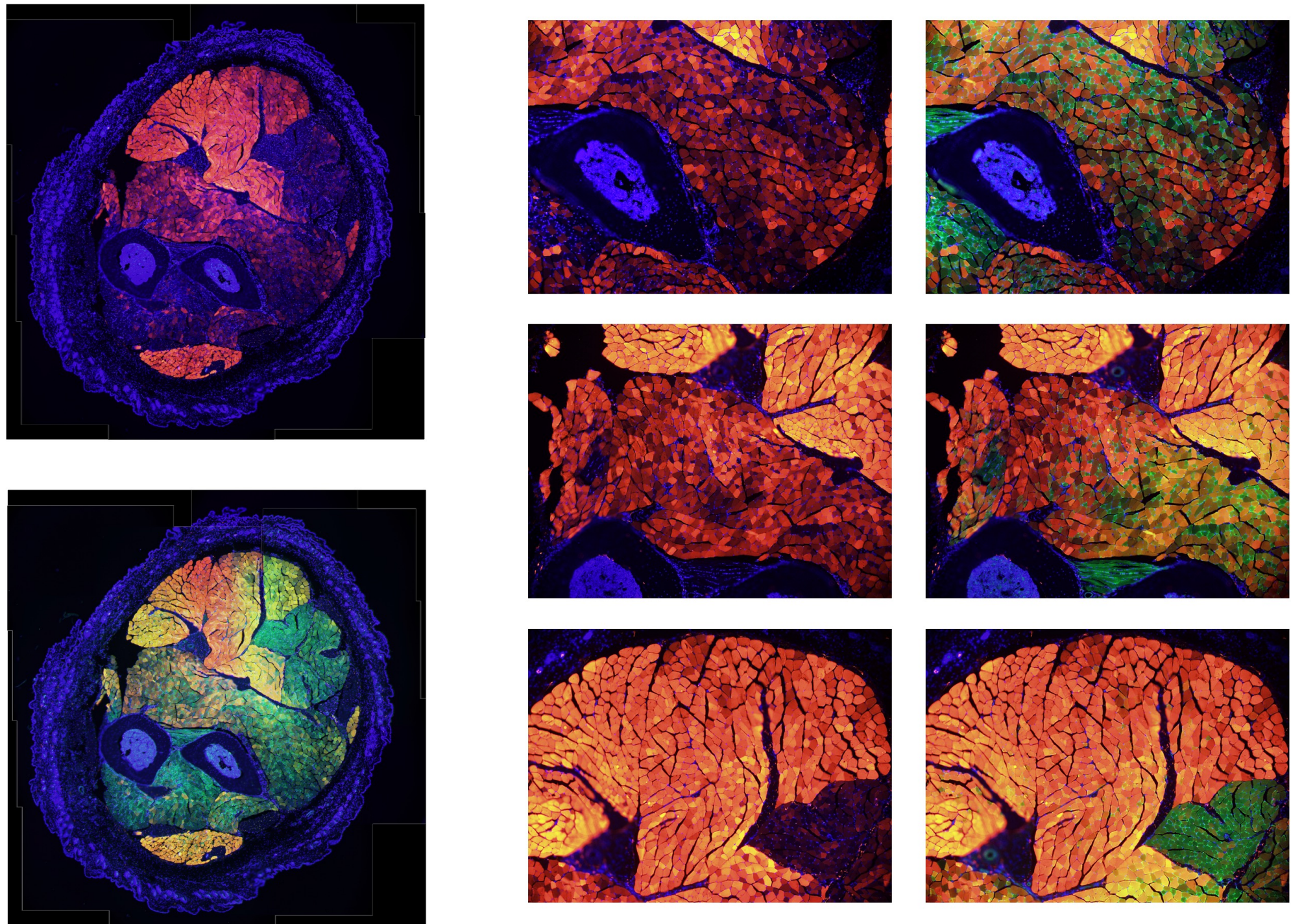


Figure S4. Hoxa11 lineage 24 weeks after reporter induction. $Hoxa11^{CreERT2/+}; ROSA^{LSL-tdTomato/+}$ mice were given 5mg tamoxifen at 8 weeks of age and collected 24 weeks (6 months) later. A full cross-section with and without background (green) show many Hoxa11iTom+ (red) muscle fibers. Close ups with and without background depict high levels of tdTomato within muscle fibers.

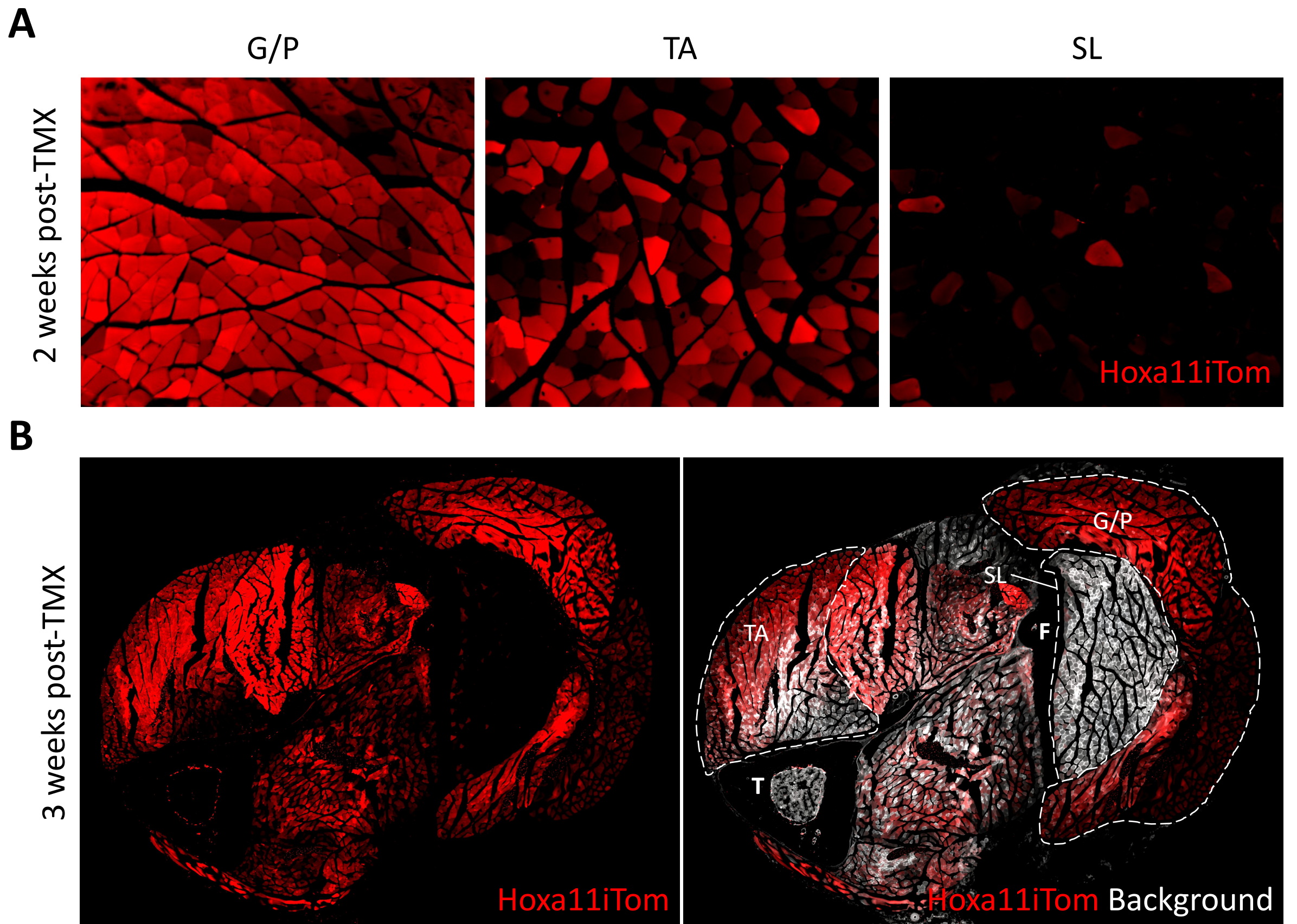


Figure S5. Hoxa11 lineage differentially contributes to hindlimb muscles. (A) Hindlimb muscles taken from Hoxa11iTom animals 2 weeks after tamoxifen treatment show different levels of lineage contribution in the Gastrocnemius/Plantaris (G/P), Tibialis Anterior (TA), and Soleus (SL). (B) A whole hindlimb cross-section from an animal 3 weeks after the start of lineage labeling shows variable tdTom expression in muscles of the hindlimb. T and F mark the tibia and fibula, respectively. Muscles shown in A are outlined and labeled in B.

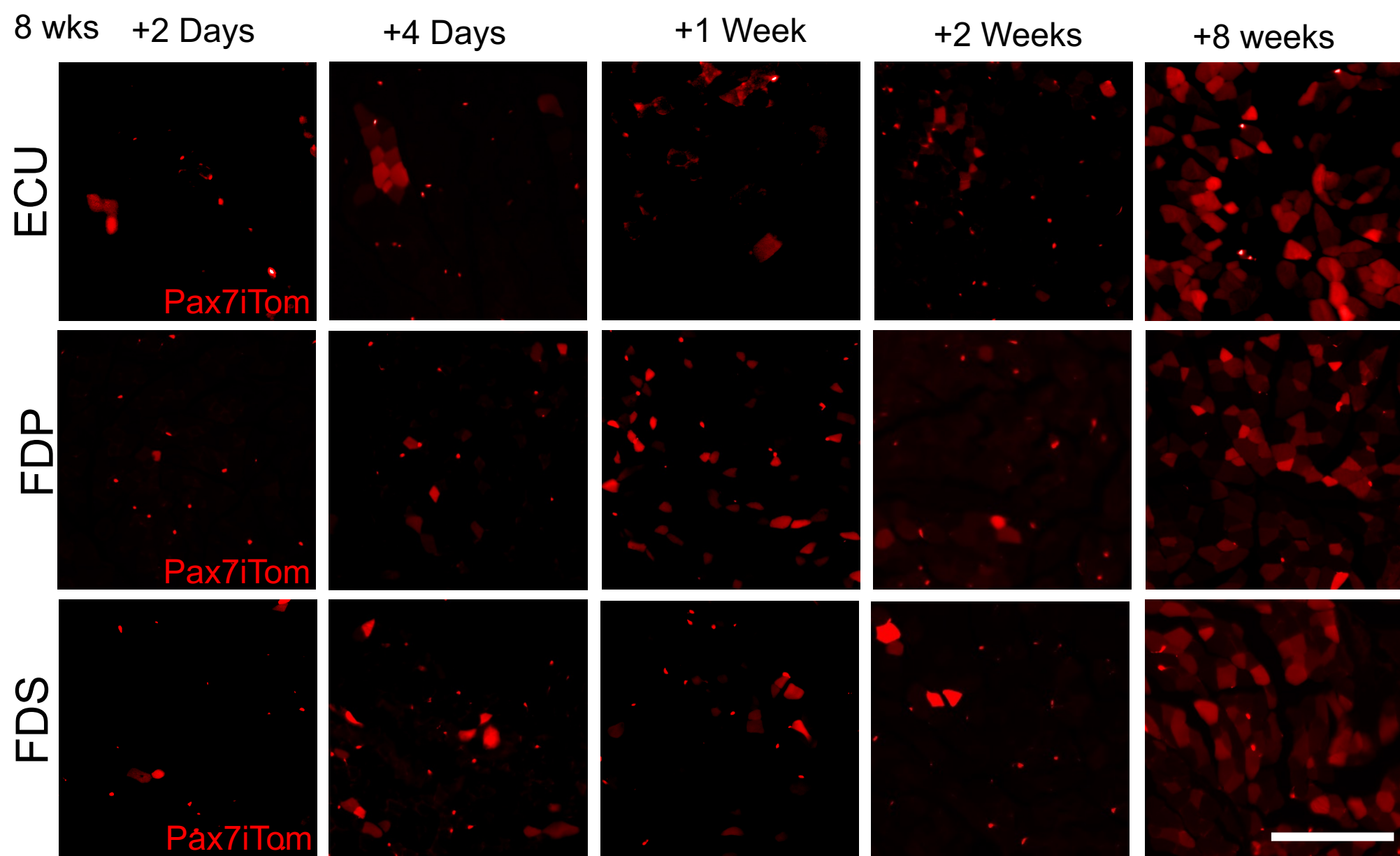


Figure S6. Pax7iTom lineage in the forelimb muscles. *Pax7CreERT2; ROSALSL-TdTomato* (Pax7iTom) mice were given a single intraperitoneal injection of 5 mg tamoxifen at 8 weeks of age and collected at 2 days, 4 days, 1 week, 2 weeks, and 8 weeks after tamoxifen induction. Images of the Extensor Carpi Ulnaris (ECU), Flexor Digitorum Profundus (FDP) and Flexor Digitorum Sublimis (FDS) muscles show tdtom⁺ myofibers as well as tdTom⁺ satellite cells.

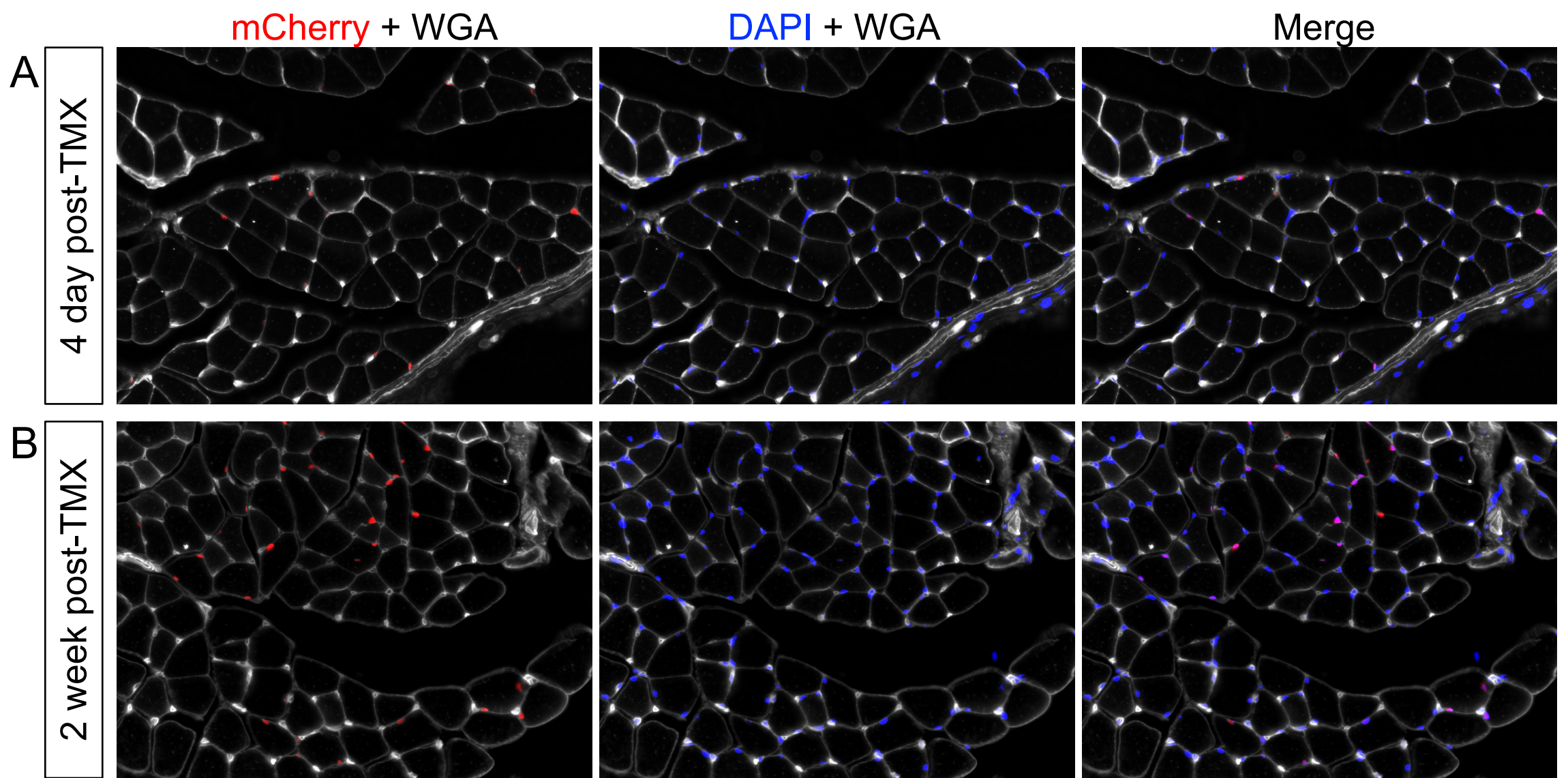


Figure S7. Hoxa11iH2BmCherry labeled nuclei overlap with nuclear stain. H2BmCherry expression in nuclei seen in figure 5 was confirmed with DAPI nuclear stain in images 4 days (**A**) and 2 weeks (**B**) post tamoxifen.

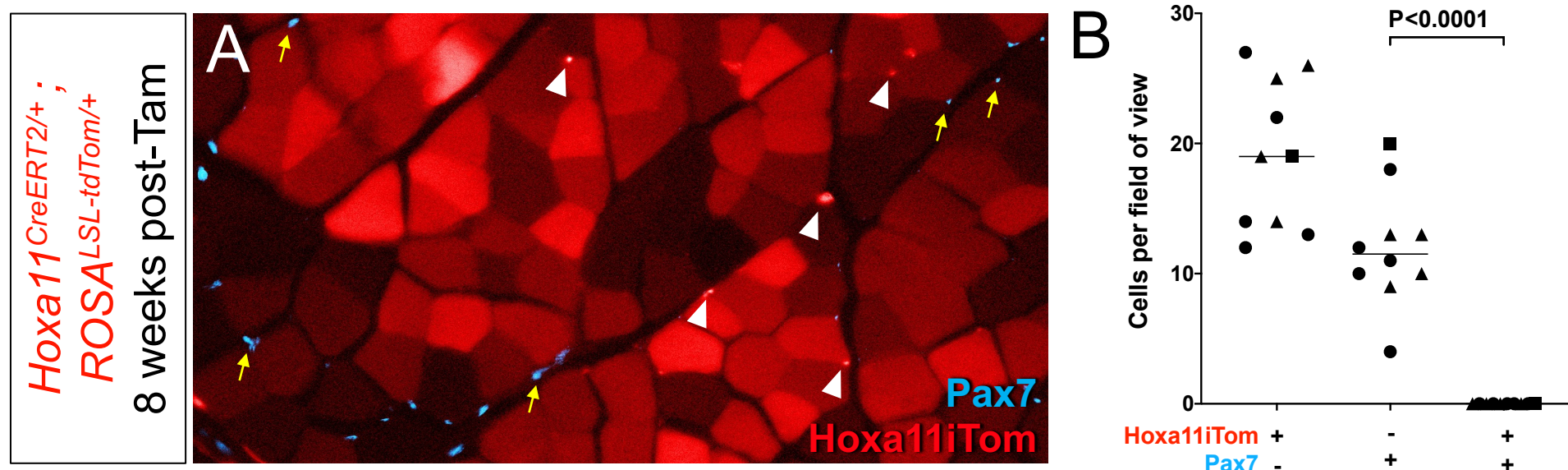


Figure S8. Hoxa11 lineage does label satellite cells 8 weeks post-induction of lineage reporter. (A) Forelimb muscle sections from animals 8 weeks (dosing at 8 weeks of age, collection at 16 weeks of age) after the start of lineage labeling were stained for Pax7 (cyan, yellow arrows) and analyzed for overlap of Hoxa11iTom (red, arrowheads) and Pax7. (B) Quantification shows no Hoxa11iTom+/Pax7+ cells were observed through forelimb muscles.

Table S1. Antibodies

Name	Source	Catalog Number	Dilution	Antigen retrieval
anti-GFP	Aves Labs	GFP-1010	1:200	No
anti-Twist2	Abcam	ab66031	1:200	No
anti-PDGFRa	Abcam	ab61219	1:50	No
anti-Tcf4	Cell Signaling	2569S	1:100	No
WGA-647	Invitrogen	W32466	1:250	No
WGA-488	Invitrogen	W11261	1:250	No
anti-Pax7	DSHB	Pax7-S	1:10	Yes
anti-Laminin	Sigma	L9393	1:500	No
anti-My32	Sigma	M4276	1:400	Yes
anti-PECAM1	DSHB	2H8-S	1:10	No
anti-BF-F3	DSHB	BF-F3	1:10	Yes
anti-SC-71	DSHB	SC-71	1:10	Yes
anti-Myosin (Skeletal, Slow)	Sigma	M8421	1:250	Yes
anti-Scal(Ly6A/E)-PE	BD Pharmingen	553108	1:100	No
anti-Ter119-AF700	BD-Pharmingen	560508	1:100	No
anti-CD31-PE-CF594	BD-Horizon	563616	1:100	No
anti-ITGA7-AF647	AbLab	67-0010-05	1:100	No
anti-CD45-AF700	Invitrogen, eBioscience	56-0451-80	1:100	No
anti-CD106(VCAM1)-PE/Cy7	Biolegend	105719	1:40	No
Alexa-488 Donkey anti-Chicken	Jackson ImmunoResearch Labs	016-580-084	1:500	No
Alexa-555 Donkey anti-Rabbit	Invitrogen	A31572	1:500	No
Streptavidin-AF647	Invitrogen	S21374	1:500	No